frontiers | Frontiers in Marine Science

TYPE Original Research
PUBLISHED 06 August 2024
DOI 10.3389/fmars.2024.1432566

OPEN ACCESS

EDITED BY
Jianfeng Feng,
Nankai University, China

REVIEWED BY
Yanbin Li,
Ocean University of China, China
Peng Zhang,
Guangdong Ocean University, China

*CORRESPONDENCE
Dawei Pan
dwpan@yic.ac.cn

RECEIVED 14 May 2024
ACCEPTED 19 July 2024
PUBLISHED 06 August 2024

CITATION
Rahman MA, Pan D, Lu Y and Liang Y (2024) Spatial-temporal distribution and eutrophication evaluation of nutrients and trace metals in summer surface seawater of Yantai Sishili Bay, China.
Front. Mar. Sci. 11:1432566.
doi: 10.3389/fmars.2024.1432566

Spatial-temporal distribution and eutrophication evaluation of nutrients and trace metals in summer surface seawater of Yantai Sishili Bay, China

Md. Abdur Rahman[1,2], Dawei Pan[1,2]*, Yuxi Lu[1,2] and Yan Liang[1,2]

[1]CAS Key Laboratory of Coastal Environmental Processes and Ecological Remediation, Shandong Key Laboratory of Coastal Environmental Processes, Research Center for Coastal Environment Engineering Technology of Shandong Province, Yantai Institute of Coastal Zone Research, Chinese Academy of Sciences, Yantai, China, [2]College of Marine Science, University of Chinese Academy of Sciences, Beijing, China

Due to coastal development expansion, an increasing influx of pollutants enters the sea through riverine input and land runoff, threatening coastal ecosystems and posing a risk of eutrophication. In this study, trace metals (Fe, Mn, Cu, and Zn), and nutrients (constituents of N, P, and Si) were assessed in the summer surface seawater of Yantai Sishili Bay (YSB), Northern China focusing on the determination of concentration, spatial-temporal distribution and sources identification, while exploring their correlations. It also aimed to clarify the eutrophication status and evaluate the linear relationships between eutrophication, trace metals, and nutrients in YSB. Over three years (2021–2023), the total dissolved concentrations of Fe, Mn, Cu, and Zn ranged from 4.79–26.71, 0.19–6.41, 0.26–1.53, and 0.74–13.12 μg/L, respectively. Concurrently, nutrient concentrations including NO_2^-, NO_3^-, NH_4^+, PO_4^{3-}, and DSi exhibited a range of 0.37–11.66, 2.04–178.30, 1.69–70.01, 0.02–16.68, and 0.02–0.71 μg/L respectively. These concentrations revealed a gradual decrease from nearshore to offshore and the temporal variation also showed significant patterns from year to year, indicating distinct regional variations. The primary contributors to the trace metals and nutrients in the study region were recognized as external contributions stemming from natural, anthropogenic, and atmospheric deposition through correlation and principal component analysis. More specifically, riverine input and coastal farming contributed large amounts of nutrients to coastal waters, threatening a potential risk of eutrophication. The eutrophication evaluation expressed below the mild eutrophication level and was far lower than the other global and Chinese bays. The linear correlation between eutrophication and trace metals revealed a weak positive correlation but a significant correlation with nutrients. Despite the absence of

significant eutrophication in the bay, potential risks were identified due to identifiable sources of nutrient and trace metal inputs. The findings provided insights to guide efforts in preventing and mitigating coastal eutrophication, as well as nutrient and trace metal pollution, in coastal cities.

KEYWORDS

trace metals, nutrients, eutrophication, spatial-temporal distribution, surface seawater

1 Introduction

Eutrophication has been recognized as a primary cause of algal bloom (Manic et al., 2024) and that refers to the phenomenon where the rapid proliferation of algae in oceanic waters, stimulated by the enrichment of nutrients, disrupts the equilibrium and stability of the marine ecosystem, impacting the seawater quality (Garmendia et al., 2012). This abnormal surge in primary productivity, particularly the proliferation of phytoplankton, serves as the primary substance for eutrophication (Pavlidou et al., 2015). As the marine economy expands swiftly and coastal zone development intensifies, the discharge of significant volumes of industrial effluents, aquaculture waste including nitrogen, phosphorus, and to some extent silica, household sewage, and the application of pesticides and fertilizers continuously introduce nutrients into coastal waters, thus fueling the rapid growth of phytoplankton (Islam and Tanaka, 2004; Manic et al., 2024). Phytoplankton is a significant constituent of the marine food web, particularly during the spring and summer seasons (Deppeler and Davidson, 2017) and the pivotal driver of trace metals and nutrient cycles (Sunda and Huntsman, 2000). The variations in the concentration and ratio of major nutrients and trace metals can result in diverse plankton community compositions, potentially leading to the formation of algal blooms (Manic et al., 2024).

Nutrients such as nitrogen (N) and phosphorus (P) are essential for the vital life processes of marine phytoplankton and are also the primary limiting factors influencing the growth. Nitrogen plays an essential metabolic role in phytoplankton physiology, acting as a foundational element for various cellular components such as nucleic acids, proteins, and chlorophyll, which are vital for algal growth and biomass production (Yodsuwan et al., 2017; Reich et al., 2020). Various nitrogen enrichment experiments have observed high cell densities and accelerated growth rates of different microalgal species (Yodsuwan et al., 2017; Longo et al., 2020). Additionally, shifts in phytoplankton community structure were observed due to elevated nutrient input, primarily N (Li et al., 2015b). Similarly, P plays a critical role in cellular metabolism, especially in processes involving energy transfer, nucleic acid synthesis, and the structure of cell membranes (Wagner et al., 2021). Moreover, P is integral to cell membranes, phospholipids, and diverse cellular molecules that enhance the integrity and fluidity of cell membranes. These metabolic roles underscore its importance as a limiting nutrient in marine ecosystems, impacting phytoplankton productivity and ecosystem dynamics (Lin et al., 2016; Paerl et al., 2016). Additionally, silicon (Si) is an indispensable nutrient for the growth of diatoms in coastal waters (Cao et al., 2020) that exerts a substantial influence on the community structure of phytoplankton (Derry et al., 2005). Si plays a more species-specific role in phytoplankton, particularly in diatoms. It acts as a structural component of their frustules, which are external siliceous cell walls providing mechanical support and protection from predators. These siliceous structures also control the uptake and transport of essential nutrients such as N, P, and C through specialized silica transporters (Martin-Jézéquel et al., 2000). Si metabolism is intricately connected to photosynthesis and carbon fixation processes in phytoplankton, thereby influencing primary productivity and the biogeochemical cycling of nutrients in aquatic ecosystems (Yool and Tyrrell, 2003; Tréguer and De La Rocha, 2013).

In parallel, trace metals exist in various chemical forms, impacting their chemistry, biological accessibility, and role as limiting nutrients (Sunda and Huntsman, 1998). Most metals exist as cations bound to inorganic or organic ligands. Essential trace elements like iron (Fe), manganese (Mn), copper (Cu), and zinc (Zn) can exist in multiple oxidation states, leading to diverse energy requirements and reaction rates that influence their bioavailability (Sunda, 1994; John and Sunda, 2019). The chemical forms of these trace metals in the water column influence their biological accessibility for phytoplankton uptake and assimilation (Sunda, 2006). Trace elements are crucial for phytoplankton growth and metabolism, leading to diverse productivities in ocean basins, coastal areas, and other aquatic ecosystems. An increasing body of research illustrates the functions of essential trace metals like Fe, Mn, Cu, and Zn as catalytic centers or structural supports in enzymes participating in various biochemical pathways (Lane and Morel, 2000; Wolfe-Simon et al., 2005; Morel et al., 2006; Ji and Sherrell, 2008; Twining and Baines, 2013). Most trace metals, such as Fe, Mn, Cu, and Zn, exhibit a nutrient-like distribution pattern akin to macronutrients (Duan et al., 2010; John and Sunda, 2019). Fe is widely acknowledged as a crucial micronutrient that restricts phytoplankton productivity in extensive oceanic areas (Rue and Bruland, 1995), primarily due to the significant Fe demands of diverse phytoplanktonic species (Morel et al., 2006). Fe serves as a cofactor for a broad array of essential enzymes crucial for diverse metabolic processes. It is essential to the structure and function of pigments, electron transport systems, and other elements of

photosynthetic machinery. The involvement of iron in enzymes critical for photosynthetic functions and various metabolic processes, including nutrient uptake and assimilation, highlights its importance in meeting the universal needs of phytoplankton for Fe (Rue and Bruland, 1995). Mn is predominantly utilized in photosynthesis, respiration, and antioxidant defense mechanisms. These roles influence the growth rates, biomass production, and ultimately the bloom dynamics of phytoplankton species (Peers and Price, 2004). The depletion of Mn leads to the restriction of the growth of phytoplankton (Facey et al., 2022). Cu has long been recognized as a vital nutrient for phytoplankton growth. Phytoplankton sensitivity to elevated Cu concentrations is evident from reduced population growth as Cu levels increase. Marine and estuarine phytoplankton populations have shown susceptibility to high Cu concentrations, exhibiting toxicity (Li, 2011; Couet et al., 2018; Long et al., 2019, 2023). Copper significantly decreases the diversity of phytoplankton and may cause reductions in phytoplankton diversity and productivity (Rodgers et al., 2010). Zn is widely recognized as a crucial micronutrient owing to its role in metalloenzymes essential for photosynthesis, protein synthesis, and antioxidant functions. Zn is observed to be indispensable for the growth of marine phytoplankton species (Rhodes et al., 2006). While numerous physiological functions supported by Zn facilitate growth and alleviate oxidative stress, elevated Zn concentrations can still hinder phytoplankton growth (Burger et al., 2022). Zn levels in the environment are significantly influenced throughout the development, duration, and decline of algal blooms. Studies have confirmed that phytoplankton uptake reduces Zn concentrations at the onset of an algal bloom (Jin et al., 2019). The intricate interaction between trace metals and nutrients suggests that their concentrations are regulated by the uptake processes in phytoplankton (Saito et al., 2017; Till et al., 2017; Middag et al., 2020). Therefore, N, P, and Si serve as pivotal indicators of eutrophication status within coastal ecosystems (Middag et al., 2020). The experimentation tools for the relationship of trace metals and nutrients with eutrophication as well as the interactions between them are needed to understand a bay's water chemistry and the changes in ratios, nutrient enrichment, algal growth, eutrophication, limiting factors, etc.

The complex interplay between eutrophication, nutrients, and trace metals in seawater represents a critical concern in contemporary marine environmental science, yet current evidence on these interactions remains insufficient and not fully comprehensible (Al-Mur, 2020). Limited temporal and spatial data, along with challenges in achieving clean sampling and accurate analytical procedures, hinder a deeper understanding of the relationships among trace metals, nutrients, and eutrophication in coastal regions. Recent scholarly endeavors have advanced our knowledge of the spatiotemporal distribution of these elements and the underlying chemistry of eutrophication (Peng, 2015; Al-Mur, 2020; Lin et al., 2020; Zhang et al., 2023; Li et al., 2024). Numerous studies have examined the distribution (Lu et al., 2020), concentration (Hong et al., 2018), species (Nakaguchi et al., 2020; Pan et al., 2020), and spatial-temporal distribution (Wang et al., 2012, 2015; Li et al., 2017; Liang et al., 2022, 2024) of trace metals. Similarly, the distribution and structure (Zhang and Gao, 2016), spatial-temporal variations (Xu et al., 2018), spatial distributions (Jiang et al., 2019) of nutrients, along with eutrophication levels (Wei et al., 2022), spatiotemporal variation (Luo et al., 2022), trophic status (Zhou and Wang, 2024), and phytoplankton variation (Wang et al., 2022) have been comprehensively studied across various coastal bays of Yellow Sea, East China Sea and Bohai Sea. Despite the growing focus on trace metals, nutrients, and eutrophication in coastal areas worldwide, the correlation among these factors remains under-documented in the coastal waters of China (Lin et al., 2020). Even within the context of studies conducted on YSB and other bays, investigations into trace metals, nutrients, and eutrophication have often been conducted separately, lacking an established linear relationship among them. Research on dissolved trace metals, nutrients, and eutrophication has predominantly concentrated on surface seawater, with scant attention paid to the differences in the distribution of these elements and their interactions across different depths. Consequently, the distribution and eutrophication risk of dissolved trace metals and nutrients in coastal areas remain poorly understood. Moreover, the intricate relationship among these factors has yet to be fully explored. This study focused on bridging these research gaps by examining the relationship between trace metals, nutrients, and eutrophication in YSB. This investigation aimed to provide a comprehensive understanding of the spatial and temporal distribution of these elements, their interactions, and the resultant eutrophication risks. The significance of this study lies in its potential to inform better management practices and policy decisions aimed at mitigating pollution and promoting the sustainability of coastal marine environments. By elucidating the complex dynamics among trace metals, nutrients, and eutrophication, this research contributed to the broader field of marine environmental science and supported efforts to preserve the ecological health of coastal waters.

YSB is situated on the southern coast of the Yellow Sea in China, where industrial, agricultural, aquacultural, fishing, tourism, mining, and other activities have been intertwined for decades. The extensive coastline offers YSB opportunities for marine development; however, it also leads to the inevitable release of pollutants into the water. Agricultural practices, aquaculture wastewater, industrial wastewater discharge, riverine inputs, and atmospheric aerosol deposition continually transport pollutants from inland areas into the ocean (Wang et al., 2016; Kelly et al., 2021). Simultaneously, Yantai serves as a significant region for fertilizer production in China, raising concerns about the extensive manufacturing and application of fertilizers (Wang et al., 2016) as well as YSB serves as an important spawning area for fish, shrimp, crab, and shellfish, and it primarily cultivates seafood for the local community, with scallops being a significant focus. Nutrients and trace metals stemming from marine economic activities, aquaculture, and inland transportation pose risks of eutrophication and ecological harm to Yantai Sishili Bay. Moreover, YSB is a partially enclosed marine area with limited water exchange capacity, imposing significant pressure on the marine ecosystem (Tang, 2004; Liu et al., 2009; Zhang et al., 2012). The effluent released from the sewage treatment plant at Xinan River and Zhifu Island, along with residues and excrement from aquatic animal feed and domestic waste from workers in aquaculture farms, all contain varying levels of nutrients and trace metals. These pollutants contribute to the contamination of the marine environment in YSB. Additionally, chemical agents are frequently employed in mariculture to manage pests, and the remnants of these substances further exacerbate nutrient

and trace metal pollution in both the marine environment and its ecosystems (Hu et al., 2007). The ongoing input of nutrients and trace metals from marine and inland sources poses a eutrophication risk to YSB (Pan et al., 2020). Exploring the trace metals, nutrients, and eutrophication levels in seawater is important for understanding the potential of marine areas like YSB. Currently, there is limited available data on nutrient and trace metal assessments in the coastal zone of YSB, leaving the eutrophication risks they pose unclear. This study collected seawater samples from YSB to assess nutrients, trace metals, and eutrophication levels. This study focused on analyzing the spatial-temporal distribution, identifying sources, and exploring correlations among nutrients (N, P, and Si) and trace metals (Fe, Mn, Cu, and Zn). It sought to clarify the eutrophication status and evaluate the linear relationships between eutrophication, trace metals, and nutrients in the coastal seawater of YSB. The findings aimed to provide insights that could guide efforts in preventing and mitigating coastal eutrophication, nutrient, and trace metal pollution in coastal cities.

2 Materials and methods

2.1 Sampling and pretreatment

Samples were taken from 12 stations throughout the summer of 2021–2023 (June–August) from the surface seawater of YSB in the Yellow Sea, China (Figure 1). When collecting water samples, GEOTRACES manual cleaning protocols are meticulously followed. Before sampling, all vessels underwent a pre-cleaning procedure that was adjusted from the cleaning method used by Li et al. (2015a) and Lu et al. (2020). All utensils were washed three times in ultra-pure water (18.2 MΩ-cm) and 10% Decon 90™ detergent (v/v) before being submerged in 10% HNO_3 and 10% HCl for 48 hours. They were then dried on a dry bench and bagged for subsequent use. Sub-boiling distillation equipment was used to pretreat all acids and ensure that they were nutrient and trace-metal grade. The remains were pure-grade reagents. Following Lu et al. (2020) guidelines, the specified sample procedure was conducted. The surface water samples (1L, 1m deep) were collected in a low-density polyethylene bottle (Nalgene™, Thermo Fisher Scientific Inc.) after being filtered with a 0.45 µm AcroPak® filter (Pall Corporation, USA). Metals that are biologically and inorganically bonded are released because of the acidification of filtered water samples. Therefore, some samples for total dissolved metals were acidified to pH< 2 with high-purity HNO_3 in a clean container and kept at 4°C until testing. The remaining samples were not acidified, and they were kept at -20°C until they were evaluated for nutrients and other physiological parameters. In addition, the COD concentration was measured using the titrimetric method.

2.2 Sampling stations

On the eastern edge of Yantai City lies the semi-closed YSB, and for this experiment, all sample sites were placed between the latitudes of 37°26'49.44"N and 37°38'10.14"N and the longitudes of 121°24'0.00"E and 121°40'27.85"E. In Supplementary Material, Supplementary Table S1 has the specifics. Figure 1 depicts the locations of 12 sampling stations (S1–S12) of this study. These were in the port regions (S4 is close to Yantai port), nearshore areas (S1–S3, where S3 is close to the Xinan River sewage treatment plant), mariculture areas (S5, S6, S8, and S9), sewage outfall sites (S7 is close to the Zhifu Island sewage treatment plant), and offshore areas (S10–S12).

2.3 Determination of total dissolved nutrients and trace metals

The seawater samples for nutrients including nitrate (NO_3^-), nitrite (NO_2^-), ammonium (NH_4^+), phosphate (PO_4^{3-}), and dissolved silicate (DSi) were processed and examined by flow injection analysis (QuAAtro, SEAL Analytical, Germany) (Liu et al., 2019) and the

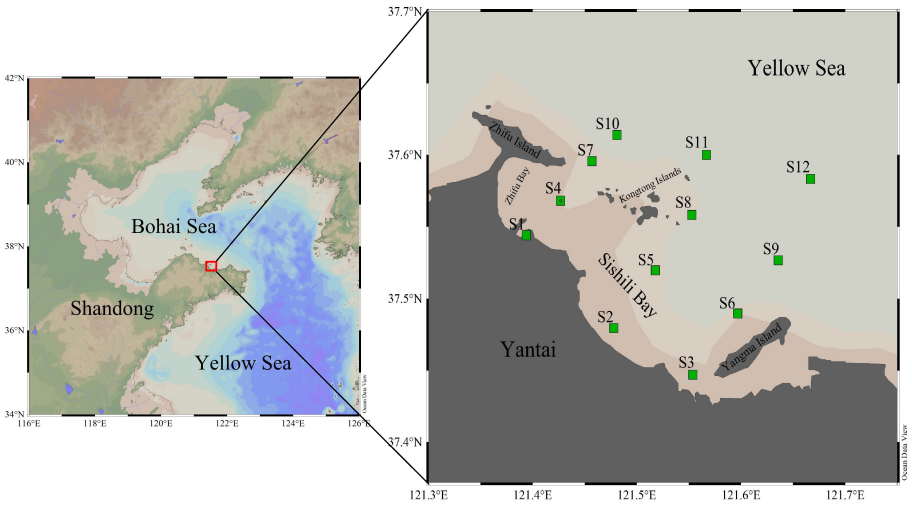

FIGURE 1
Map of the sampling location in the YSB with the green square marks as the sampling stations.

processing schematic view is presented in Supplementary Figure S1. The limits of detection were 0.02, 0.008, 0.03, 0.01, and 0.02 µmol/L for NO_3^-, NO_2^-, NH_4^+, PO_4^{3-}, and DSi, respectively (Sun et al., 2022). The concentrations of total dissolved nitrogen (TDN) were calculated as the sum of NO_3^-, NO_2^-, and NH_4^+.

The concentrations of dissolved trace metals (Fe, Mn, Cu, and Zn) were assessed using an inductively coupled plasma mass spectrometer (ICP-MS, NEXION 1000G, PerkinElmer® USA) (Lu et al., 2020; Liang et al., 2022) and the pre-processing of metal detection was done using ELSpe-2 PreCon Automatic Desalting Separation and Enrichment System (Guangzhou Prin-Cen Scientific Limited, China). The flow diagram in Supplementary Figure S2 shows the trace metals analysis process using ICP-MS. To ensure the precision of the succeeding experimental approaches, the ICP-MS method was validated. By detecting diluted 0.5 percent HNO_3 10 times with ultra-pure water, the ICP-MS technique blanks were calculated. The accuracy of the experimental detection method was confirmed which displayed the limit of detection (LOD) as 0.1, 0.909, 0.008, 0.018 µg/L and the limit of quantification (LOQ) as 0.027, 0.746, 0.032, 0.172 µg/L for Fe, Mn, Cu, and Zn, respectively, alongside the linear correlations (R^2 = 0.999). The high R^2 values and low LOD and LOQ for the analyzed elements underscore the precision and reliability of the detection technique employed in the study.

2.4 Eutrophication analysis

"Technical Regulation for Assessment of Seawater Quality Status (Trial), 2015.10" first introduced the method for calculation of the Eutrophication Index (EI) in the Bays of China (Zhou, 2018; Youping et al., 2020). The introducing formula was also used several times by numerous scholars e.g., Lin et al. (2020); Son et al. (2020), and Wang et al. (2009)for assessing the EI of seawater. The formula is presented below, followed for executing the calculation of EI in this study.

$$EI = \frac{COD \times DIN \times DIP \times 10^6}{4500}$$

Where, COD, DIN,and DIP, respectively, stand for chemical oxygen demand, dissolved inorganic nitrogen (NO_2^-+NO_3^-+NH_4^+), and dissolved inorganic phosphorus (PO_4^{3-}). Three eutrophication levels were established: mild eutrophication (1≤ EI ≤3), moderate eutrophication (3< EI ≤9), and severe eutrophication (E >9).

2.5 Data analysis

In this study, the data underwent rigorous statistical scrutiny utilizing IBM SPSS Statistics (Version 19.0) and Origin 2024 (Version 10.1). The spatial distributions of both nutrients and trace metals were meticulously crafted using Ocean Data View (Version 4.0). Delving deeper, Pearson Correlation and Principal Component Analyses (PCA) were used to evaluate the interconnections between the concentrations of dissolved nutrients and trace metals at various sampling sites within the YSB over different years (Yano et al., 2019), all expertly managed by IBM SPSS Statistics (Version 19.0) and Origin 2024 (Version 10.1) following the methodology established in prior studies (Ma et al., 2016).

3 Results and discussion

3.1 Spatial-temporal distribution of dissolved nutrients

The spatial-temporal distribution of nutrients, including NO_2^-, NO_3^-, NH_4^+, PO_4^{3-}, and DSi in selected stations from 2021 to 2023, as illustrated in Figures 2A–E. Despite variations in the patterns observed for different years across both inshore and offshore areas, a consistent characteristic emerged: concentrations decreased from nearshore to offshore regions, aligning with findings from Lin et al. (2020), suggesting a common nutrient source in the YSB. Dissolved nitrogen constituents exhibited significant variability across the YSB, with three-year mean concentrations of NO_2^-, NO_3^-, and NH_4^+ in surface seawaters ranging from 0.37–11.66 µg/L, 2.04–178.30 µg/L, and 1.69–70.01 µg/L, respectively (Supplementary Table S2). Along the coastline, concentrations decreased notably seaward, with the highest NO_2^-, NO_3^-, and NH_4^+ concentrations typically observed at stations nearest the coast, particularly S1-S8, reflecting significant human activity (Wang et al., 2012).

The highest NO_2^- concentration of 11.66 µg/L was recorded at S1 in 2023, contrasting with the lowest value of 0.37 µg/L at S12 in 2022 (Figure 2A; Supplementary Table S2). Station S1 is situated in the nearshore area with a drastic human influence pressure such as summertime fishing, tourism, local inland nutrient enrichment, etc. The yearly concentration pattern of NO_2^- exhibited erratic fluctuations (Figure 2A) with no clear directional trend but maintained a relatively stable trend, with minor fluctuations due to the increasing input sources such as industrial development, coastal farming, water transportation, etc. This kind of variability might have stemmed from factors such as microbial integrity, which could rapidly alter NO_2^- concentrations in response to changing environmental conditions (Peng, 2015). Additionally, anthropogenic sources like industrial discharges and sewage effluents might have contributed to the observed variability in NO_2^- levels (Wang et al., 2012). Similarly, station-specific extremes were observed, such as the highest NO_3^- concentration of 178.30 µg/L at S7 in 2021 due to the pressure of extensive sewage discharge from the Zhifu island sewage treatment plant and the lowest of 2.04 µg/L at S4 in 2022 (Figure 2B; Supplementary Table S2). The NO_3^- concentrations were not maintained regularity but had stable characteristics that showed a notable decreasing trend from 2021 to 2023 (Figure 2B). The stations with the highest concentration e.g., S7, were possibly influenced by factors such as effluent discharge from the nearest locality, biological uptake, and chemical inputs from the agricultural land that variations in the concentration of NO_3^- levels had been observed by the previous study of Li et al. (2024), suggesting a complex interplay of anthropogenic factors driving these changes in this kind of semi-enclosed bay.

Furthermore, the highest NH_4^+ concentration of 70.01 µg/L arose at S8 in 2023, while the lowest was 1.69 µg/L at S8 in 2022 (Figure 2C; Supplementary Table S2), indicating nitrogen

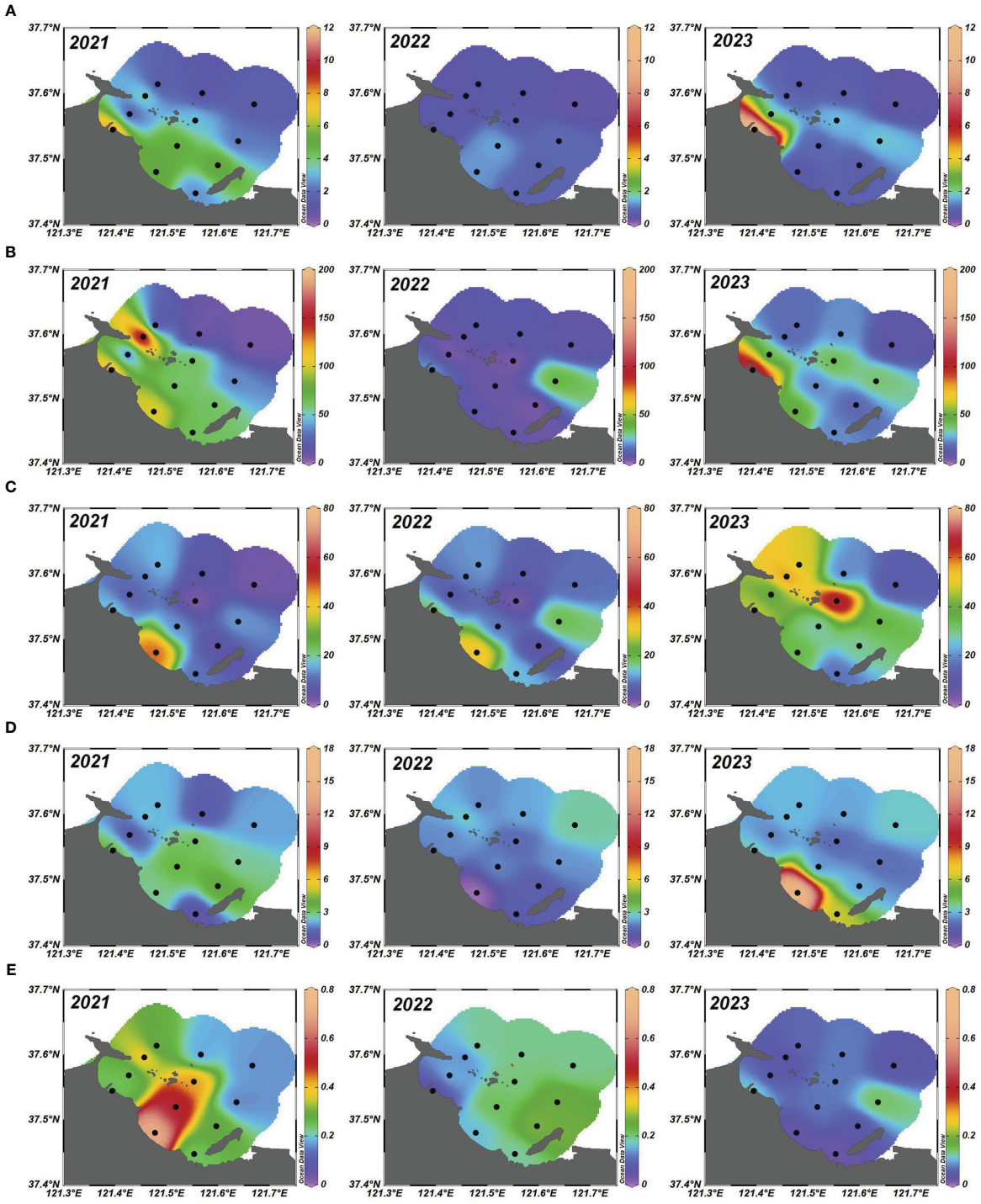

FIGURE 2
Spatial-temporal distribution of **(A)** NO_2^- (μg/L); **(B)** NO_3^- (μg/L); **(C)** NH_4^+ (μg/L); **(D)** PO_4^{3-} (μg/L) and **(E)** DSi (μg/L) from 2021 to 2023 in the summer surface seawater of YSB, China.

enrichment in the YSB that the findings agreed with the previous study of Li et al. (2024). Stations S8 with elevated NH_4^+ concentration than the other stations, were likely impacted by the extensive mariculture activities including the discharge of chemicals, food residue, wastewater from the fishermen, etc. The highest and lowest concentrations of NH_4^+ indicated in the same station could be possible due to the extension of mariculture farming or sudden changes in the nutrient input sources. As per the temporal variation, the concentration of NH_4^+ showed a consistent rise from 2021 to 2022, followed by a decline in 2023 (Figure 2C). This trend likely reflected shifts in nutrient cycling, such as microbial decomposition and organic matter breakdown, affecting NH_4^+ levels in marine ecosystems (Li et al., 2024). Additionally, human actions like wastewater release and

agricultural practices could have contributed to NH_4^+ inputs, affecting its temporal changes (Wang et al., 2012; Li et al., 2024).

The three-year mean concentrations of PO_4^{3-} in the surface seawaters of the YSB ranged from 0.02 to 16.68 μg/L, averaging 2.82 μg/L (Supplementary Table S2). Dissolved PO_4^{3-} concentrations decreased seaward over the period, except in 2021. Despite a relatively higher PO_4^{3-} concentration of 16.69 μg/L being recorded in S2 of 2023, the lowest concentration of 0.02 μg/L was also observed in S2 of 2022 (Figure 2D; Supplementary Table S2). Similar distribution patterns to previous studies (Wang et al., 2012; Li et al., 2024), suggested anthropogenic activities as the main source of PO_4^{3-} in the YSB. The same location had the lowest and highest values of PO_4^{3-} due to the yearly fluctuation of human influence in the Bay. Station S2 was dominated by fishing activities, urban runoff, sewage discharge, etc. that were implicated in PO_4^{3-} distribution. Average PO_4^{3-} concentrations across the 12 sampling stations were relatively low, consistent with findings from studies in the coastal water of the Bohai Sea by Lin et al. (2020), indicating higher N and lower P concentrations in these areas. Prior research indicates that mariculture elevates N and P levels in coastal waters, with NO_3^- constituting a substantial portion of inorganic N, consistent with the current study's results (Kang and Xu, 2016). With considering the temporal variation the PO_4^{3-} remained relatively stable across the three years, with only minor variations (Figure 2D). This stability was likely due to phosphorus's conservative behavior in marine systems, where it tends to bind to particles and sediments, resulting in slower turnover rates compared to nitrogen compounds (Redfield, 1958). However, localized events such as sediment disturbance and phytoplankton blooms could still have affected PO_4^{3-} dynamics (Al-Mur, 2020; Li et al., 2024).

Similarly, DSi concentrations remained relatively steady over the three years, with slightly significant trends observed (Figure 2E) that similarly agreed with the previous study of Wang et al. (2012). However, in this study, DSi levels appeared to stay within a narrow range, indicating resilience to external disruptions. The three-year average concentrations of DSi ranged from 0.02 to 0.71 μg/L, with an average of 0.19 μg/L (Supplementary Table S2). DSi in inshore waters exhibited significant variation along the coast and decreased notably seaward. The distribution pattern of DSi in inshore waters closely paralleled that of other nutrients, suggesting influences from both natural and human activities (Cao et al., 2020). The varying distribution of DSi in the study area suggests that its source is primarily indigenous, originating from diatom-produced biogenic silicate, rather than being primarily introduced from external sources such as drains. This indicates a significant role of diatom activity in shaping the distribution of silicate content (Verschuren et al., 1998). The highest DSi concentration of 0.71 μg/L persisted in S2 in 2021, whereas the lowest value of 0.02 μg/L occurred in S3 in 2023 (Supplementary Table S2). Silicate minerals, originating from the crust, are typically less influenced by human activities (Wang et al., 2012). However, construction and industrialization along the YSB banks may have released more silicate minerals into the water system, as these activities involve excavating clay and rock, major constituents of silicate minerals, from underground to the surface. The yearly variation of NO_2^-, NO_3^-, NH_4^+, PO_4^{3-}, and DSi in marine environments was influenced by various factors, including natural processes and human activities (Wang et al., 2012). While some nutrients showed clear trends over time, others exhibited more erratic fluctuations, underscoring the complexity of nutrient cycling dynamics.

3.2 Spatial-temporal distribution of dissolved trace metal

The portrayal of the spatial-temporal distributions of trace metals in the summer surface seawater of YSB from 2021 to 2023 is depicted in Figures 3A–D. Marine organisms accumulate trace metals such as Fe, Mn, Cu, and Zn in their tissues and bones, as these elements are essential for biological growth and are commonly referred to as trace nutrients (Liang et al., 2022). Supplementary Table S2; Figures 3A, B showcased the spatial temporal distribution of dissolved Fe and Mn contents along the YSB coast. The concentrations were lower at nearshore stations than at offshore stations. The concentration of dissolved Fe fluctuated from 4.79 μg/L at S1 during 2022 to 26.70 μg/L at S8 during 2021. Notably, S8, located near sewage outfall sites of Zhifu Island sewage treatment plant and mariculture activities, exhibited higher Fe concentrations, potentially attributed to these activities (Pan et al., 2020), suggesting that sewage from the aquaculture area carried by ocean currents may be responsible for the higher Fe. The average Fe concentration during the study period stood at approximately 12.70 μg/L. According to the yearly temporal variation, Fe levels displayed a certain range of values across the sampled stations in 2021, indicative of localized influences such as geological characteristics and point sources. However, as the years progressed, there appeared to be a general decrease in Fe concentrations in 2022, followed by a slight recovery or stabilization in 2023. This temporal pattern may have reflected changes in sedimentation rates, redox conditions, or input sources over time. Notably, the observed trends in Fe concentrations aligned with findings from a previous study (Pan et al., 2020), which highlighted the dynamic nature of Fe cycling in aquatic environments and its sensitivity to environmental factors. The results showed that Fe concentrations were lower than in the other bays and in previous studies in this Bay (Hong et al., 2018; Pan et al., 2020). Unlike total dissolved Mn, Cu, and Zn a reverse distribution pattern was found for total dissolved Fe, indicating that the source of Fe might differ from the sources of Mn, Cu, and Zn.

In parallel, Mn concentrations in the study area ranged from 0.19 μg/L at S9 during 2021 to 6.41 μg/L at S8 during 2022. Over the consecutive three years, the average Mn content was 1.24 μg/L. Mn displayed considerable variability, with approximately six to eightfold differences between their high and low concentrations. Generally, the dissolved Mn concentrations indicated lower values in the YSB compared to other coastal areas such as Zhanjiang Bay (Hong et al., 2018) and the East China Sea (Nakaguchi et al., 2020). Mn concentrations also showed a distinct temporal dynamic across the studied years (Figure 3B) that indicated Mn levels varied considerably among stations in 2021, suggesting spatial heterogeneity in Mn sources and cycling processes. However, over the subsequent years, there seemed to be a convergence towards

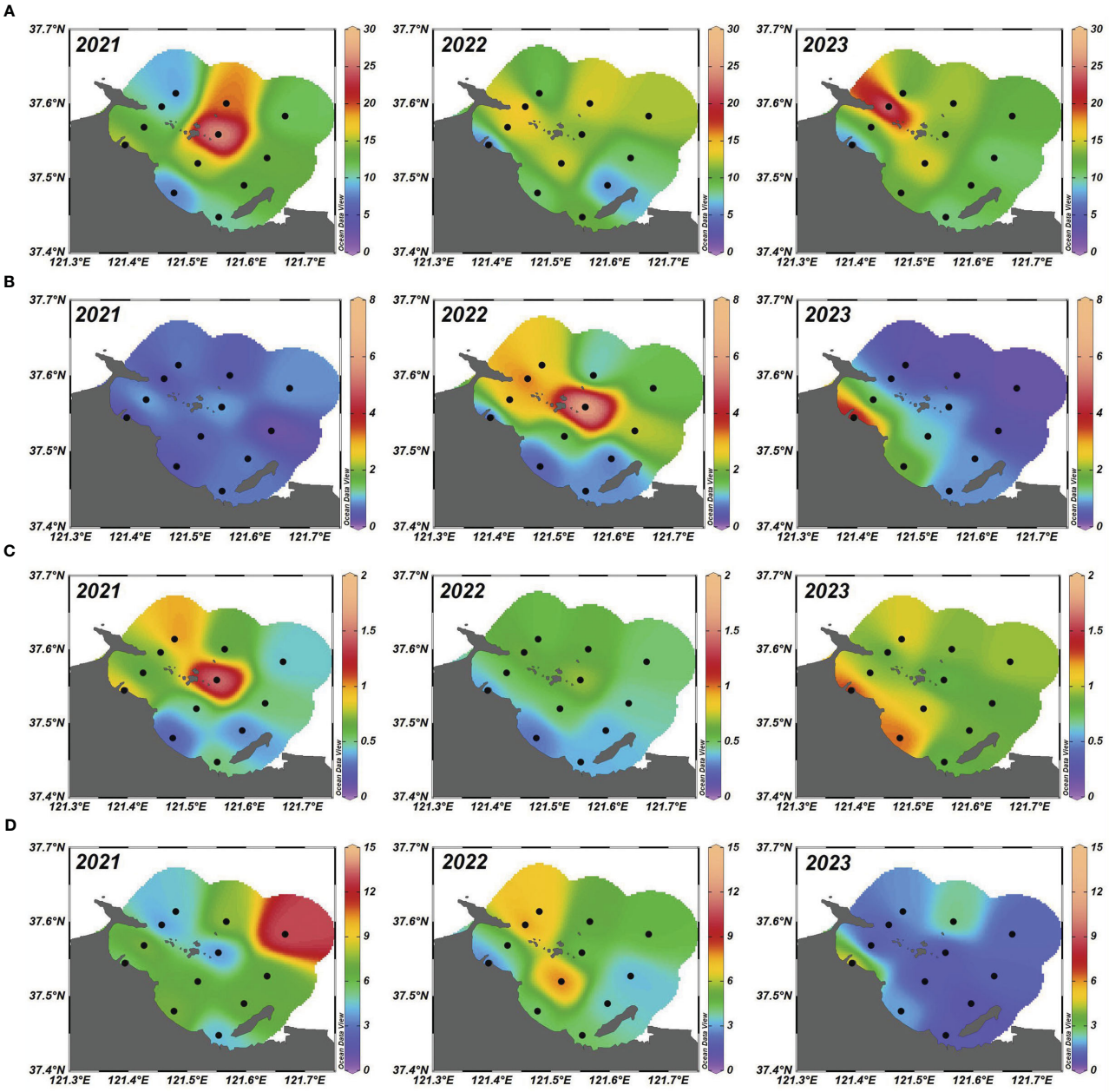

FIGURE 3
Spatial-temporal distribution of **(A)** Fe (μg/L); **(B)** Mn (μg/L); **(C)** Cu (μg/L) and **(D)** Zn (μg/L) from 2021 to 2023 in the summer surface seawater of YSB, China.

more uniform Mn concentrations, with some stations exhibiting decreases while others remained relatively stable. This temporal variability in Mn concentrations underscored the complex interplay between sedimentary processes, redox dynamics, and anthropogenic inputs. These findings resonated with those reported in the literature (Nakaguchi et al., 2020) emphasizing the importance of understanding Mn cycling in aquatic ecosystems and its implications for water quality management. The spatial-temporal distribution of dissolved Cu in the study area is illustrated in Figure 3C. Throughout the study period, dissolved Cu concentration values oscillated between a minimum of 0.26 μg/L at S2 and a maximum of 1.53 μg/L at S8 during 2021. The average concentrations of dissolved Cu over the three years were recorded at 0.70 μg/L (Supplementary Table S2). The highest concentrations of Mn and Cu were observed at station S8, adjacent to mariculture areas, suggesting contributions from food and chemical residues, as well as household waste from aquaculture activities. Atmospheric deposition may have also played a role in the elevated Mn and Cu levels at offshore stations (Pan et al., 2020; Liang et al., 2024). The temporal fluctuations in Cu concentrations were also notable over the study period, as depicted in Figure 3C. Cu levels exhibited variability across stations in 2021, likely reflecting diverse sources such as industrial discharges and urban runoff. However, by 2022, there appeared to be a general increase in Cu concentrations at

several stations, possibly indicating changes in anthropogenic inputs or environmental conditions (Li et al., 2024). By 2023, Cu concentrations exhibited mixed trends, with some stations showing further increases while others experienced declines or stability. These temporal patterns in Cu concentrations highlighted the dynamic nature of Cu cycling in aquatic systems and its vulnerability to human activities. These observations were in line with previous studies (Pan et al., 2020; Liang et al., 2024) highlighting the significance of Cu contamination in aquatic ecosystems and the need for effective pollution control measures.

Dissolved Zn at the coastal study sites is displayed in Figure 3D. The concentration of Zn ranged from 0.74 µg/L at S6 during 2023 to 13.12 µg/L at S12 during 2021. Station S12 was located offshore areas, where the dry-wet deposition of atmospheric aerosols was the main external source of Zn (Zheng et al., 2003). This indicates that atmospheric deposition may be the cause of the higher Zn levels. However, station S12 was close to the aquaculture zone, suggesting that sewage from the aquaculture area carried by ocean currents may be responsible for the higher Zn (Pan et al., 2020). The three-year average concentration of dissolved Zn was 4.31 µg/L (Supplementary Table S2). Overall, biological factors strongly influenced the bioaccumulation of metals, with Zn being naturally abundant and known to contaminate residues from food waste, pesticides, and anti-corrosion paints (Li et al., 2024). Zn concentrations also demonstrated temporal variation across the three years, reflecting changes in environmental conditions and anthropogenic influences (Figure 3D). Zn levels exhibited spatial heterogeneity among stations in 2021, suggesting localized sources and transport pathways. However, by 2022, there seemed to be a general decrease in Zn concentrations across the sampled stations, followed by mixed trends in 2023, with some stations showing increases while others experienced declines. These temporal patterns in Zn concentrations underscored the complex interplay between natural processes and human activities shaping Zn cycling in aquatic environments. These findings were consistent with previous research (Pan et al., 2020; Liang et al., 2022; Li et al., 2024), emphasizing the need for comprehensive monitoring and management strategies in aquatic ecosystems.

Overall, the temporal variation of Fe, Mn, Cu, and Zn concentrations across the years 2021, 2022, and 2023 revealed dynamic patterns indicative of changing environmental conditions and anthropogenic influences. The comparison of these elements over the three years unveiled shifts in concentration levels, hinting at underlying environmental processes and potential anthropogenic influences. While each element's behavior varied, collectively, they offered insights into ecosystem health and water quality dynamics. The YSB's shallow water depth and poor exchange capacity, coupled with its relatively aged water body, may have facilitated desorption or remineralization processes, leading to the migration of metals from solid phases into the water body (Kalnejais et al., 2010; Lü et al., 2010). Resuspension resulting from these processes likely contributed to increased metal concentrations in the area. Additionally, spatial differences in metal content may have been influenced by marine disasters (Liang et al., 2022).

3.3 Correlation between dissolved trace metals and nutrients

Interpreting the analyzed data spanning three years (2021–2023) in the seawater of YSB revealed dynamic interactions among various parameters, including concentrations of trace metals (Fe, Mn, Cu, and Zn), nutrients (NO_3^-, NO_2^-, NH_4^+ and PO_4^{3-}), and DSi (Supplementary Table S3; Figure 4). The Pearson correlation matrix demonstrated the relationships between these components across three years, reflecting changes in their concentrations and potential influences on marine ecosystems. Fe, a crucial micronutrient, showed consistent positive correlations with Mn and Cu throughout the years. This suggested potential co-occurrence or shared sources of these metals in seawater, likely originating from both natural processes and anthropogenic inputs such as industrial discharge or atmospheric deposition (Pan et al., 2020). The positive correlation between Fe and Mn indicated their association with particulate matter or organic ligands, influencing their solubility and bioavailability (Crawford et al., 2003; Saito et al., 2005). The positive correlation of Cu with Fe and Mn stemmed from similar sources or redox cycling processes involving these metals. Zn exhibited variable correlations with other parameters across the years, ranging from negative to positive values. In 2021, Zn showed

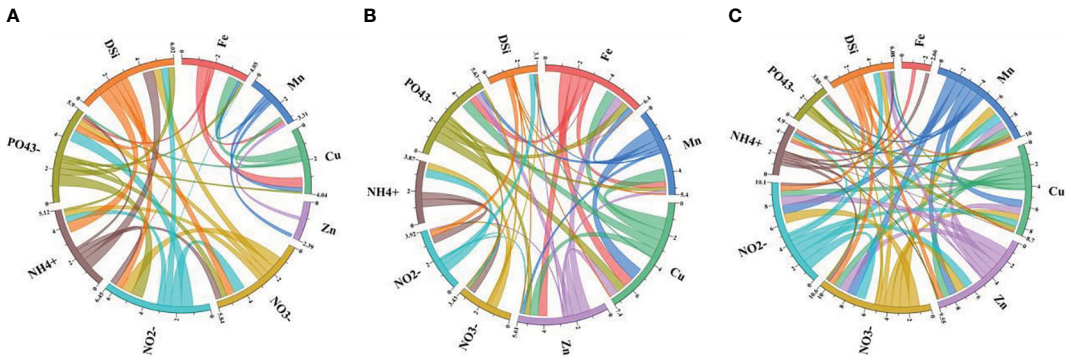

FIGURE 4
Correlation matrix of **(A)** 2021; **(B)** 2022; and **(C)** 2023 for the concentrations of dissolved nutrients and trace metals in the surface seawater of YSB, China.

weak negative correlations with Fe, Mn, and Cu, suggesting possible antagonistic interactions or independent sources. However, in 2022 and 2023, the correlations of Zn with Fe, Mn, and Cu became positive, implying potential shifts in sources or chemical speciation influenced by environmental factors such as pH, salinity, or organic complexation (Pan et al., 2020). NO_3^- and NO_2^- displayed consistent positive correlations across the years, indicating their co-occurrence and shared sources, primarily from anthropogenic activities such as agricultural runoff, wastewater discharge, or atmospheric deposition (Lin et al., 2020). The strong positive correlation between NO_3^- and NO_2^- suggested similar sources and transformation pathways, reflecting the dynamics of nitrogen cycling in seawater influenced by biological processes like nitrification and denitrification (Zhang and Gao, 2016). NH_4^+ concentrations showed moderate to strong positive correlations with NO_3^- and NO_2^- across the years, suggesting potential interactions between organic matter degradation, microbial activity, and nutrient cycling processes in seawater. NH_4^+ may serve as a substrate for nitrifying bacteria, contributing to the production of NO_3^- and NO_2^-. NH_4^+ serves as the primary nitrogenous byproduct arising from the breakdown of nitrogen-containing organic matter through microbial decay. It is also a significant excretion product for both invertebrates and vertebrates. Additionally, ammonia represents a crucial inorganic nitrogen form, favored by aquatic plants for uptake (Faragallah et al., 2010). Elevated levels of ammonium could result in increased phytoplankton productivity, particularly if these organisms preferentially utilize NH_4^+ over NO_3^- (Dugdale et al., 2007). The positive correlations between NH_4^+ and trace metals (Fe, Mn, Cu, and Zn) hinted at potential associations with organic ligands affecting their solubility and bioavailability in seawater (Li et al., 2024). PO_4^{3-} concentrations exhibited variable correlations with other parameters over the years, indicating potential influences from both natural processes and anthropogenic inputs such as agricultural runoff, sewage discharge, or atmospheric deposition (Wang et al., 2012). The positive correlations between PO_4^{3-} and trace metals (Fe, Mn, Cu, and Zn) from 2021 to 2023 suggested potential associations with particulate matter enhancing their mobility and availability in seawater. However, in 2022, PO_4^{3-} showed significant positive correlations with Cu, possibly due to shifts in nutrient dynamics influenced by environmental factors or biological uptake processes (Wang et al., 2012; Li et al., 2024). Besides this, the negative correlation of PO_4^{3-} with Mn (2021) and Fe (2023) possibly indicated that increasing phosphate concentrations could have inhibited the bioavailability or solubility of Mn and Fe due to complexation reactions or precipitation, influencing their distribution in the YSB (Peng, 2015; Lin et al., 2020). Dissolved silica (DSi) concentrations demonstrated consistent positive correlations with trace metals (Fe, Mn, Cu, Zn) across the years, indicating potential interactions with siliceous organisms, such as diatoms or sponges, which utilize DSi for biomineralization processes (Cao et al., 2020). The positive correlations between DSi and trace metals suggested co-occurrence or shared sources influenced by processes like dissolution of silicate minerals or desorption from sedimentary particles (Wang et al., 2012). In summary, the interpretation of seawater chemistry data from 2021 to 2023 highlights dynamic interactions among metals, ions, and dissolved silica, reflecting the complex interplay of natural processes and anthropogenic influences in marine environments. Understanding these relationships is crucial for assessing the health and resilience of marine ecosystems.

Principal Component Analysis (PCA) is a powerful statistical technique used to reduce the dimensionality of complex datasets while retaining as much of the original information as possible (Li et al., 2000). The study focused on analyzing correlations and potential sources of various dissolved trace metals and nutrients in surface seawater over multiple years of monitoring. To delve deeper into the underlying drivers and uncover correlations among the raw variables, two principal components (PCs) with eigenvalues greater than 1 were extracted from the raw data through PCA (Supplementary Table S4; Figure 5). PC1, accounting for 83.5% of the total variance, primarily reflected the dominance of nutrient concentrations (NO_3^-, NH_4^+, PO_4^{3-}) in the seawater of YSB, with strong positive loadings for NO_3^- (0.99320) and NH_4^+ (0.10619), indicating their significant contributions to the variability captured by PC1. This suggested that PC1 represented the nutrient enrichment status of seawater, potentially influenced by anthropogenic inputs such as agricultural runoff or wastewater discharge, as well as natural processes like biological nutrient cycling (Wang et al., 2012; Li et al., 2024). Waterways acted as channels for human-caused contamination, releasing waste, and industrial and aquafarming toxins into marine environments (Pan et al., 2020). Moreover, internal rejuvenation from the breakdown of particle-based organisms and dispersion from seabed sediment pore water played a role in spreading metals and nutrients. The negative loadings for Fe (-0.00331), Mn (-0.00399), and Zn (-0.00098) on PC1 indicated their weaker influence compared to nutrients, suggesting that variations in these metals were not the primary drivers of variability along PC1. The accumulation or outward transport of sediments from the Yellow River (Chen

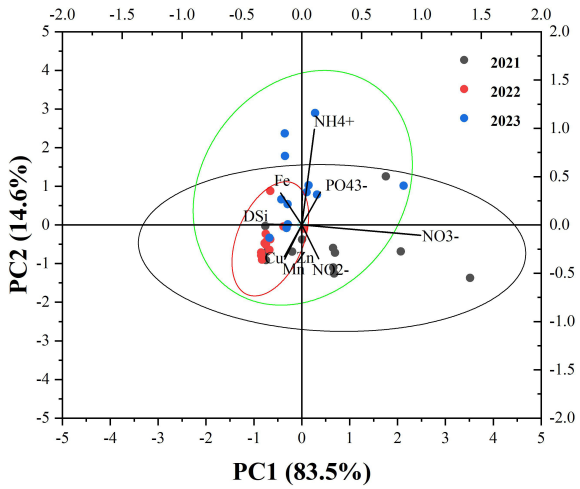

FIGURE 5
The principal component analysis loading plot of nutrients and dissolved trace metals in the summer surface seawater of YSB, China.

et al., 2013; Li et al., 2020) played an important role in the accumulation and discharge of different substances into the water, serving as a notable storage area for dissolved trace metals in the offshore regions of YSB (Gao et al., 1992; Sun et al., 2012). Many rivers emptied into the YSB, including the Guangdong River, the Han River, and the Nian River, potentially introducing anthropogenic pollution, discharged effluent, and industrial and aquaculture pollution to the ocean water (Yuan et al., 2012; Pan et al., 2020). Due to the river input into the YSB, high concentrations of trace metals were influenced and caused uneven distribution (Li et al., 2017; Pan et al., 2020). However, prior research has also suggested that the elevated atmospheric flows of trace metals and nutrients into the Chinese continental shelf, potentially exceed river inflows (Gao et al., 1992; Zhang et al., 1992). During the onset of summer, cold air currents carried crustal aerosols from the desert area in the northwest to the coastal regions in the east, notably impacting the atmospheric quality of the Yellow Sea (Gao et al., 1992).

On the other hand, PC2, explaining 14.6% of the total variance, captured additional nuances in seawater, primarily reflected by the loadings of NO_3^- (-0.10616) and NH_4^+ (0.99039). The negative loading for NO_3^- on PC2 suggested an inverse relationship with NH_4^+, indicating potential nitrogen cycling processes such as denitrification or biological uptake influencing the variability (Wang et al., 2012; Luo et al., 2022). The positive loading for NH_4^+ on PC2 reaffirms its importance in shaping the patterns observed in seawater chemistry, likely representing its contribution to microbial processes and nutrient dynamics (Li et al., 2024). Additionally, the negative loading for Zn (-0.08478) on PC2 suggested a potential inverse relationship with nutrient concentrations, indicating contrasting influences on seawater chemistry compared to NO_3^- and NH_4^+. Overall, the PCA results provided a comprehensive understanding of the dominant patterns and relationships among seawater parameters, highlighting the importance of nutrient concentrations (NO_3^-, NH_4^+, PO_4^{3-}) in driving variability captured by PC1, while PC2 captured additional nuances related to nitrogen cycling processes and potential influences of trace metals like Zn. Hydrodynamic elements such as coastal marine currents, runoff, and tidal movements were pivotal in the dissemination and conveyance of contaminants, encompassing trace metals, offshore. An experiment involving the release of particle tracers along the Yantai coast illustrated a route that closely mirrored the flow of predominant ocean currents (Sun et al., 2012). Consequently, PC2 probably denoted an organic origin for the discharge of trace metals and nourishing substances amidst the sway of external disruptions.

3.4 Eutrophication evaluation

3.4.1 Eutrophication index

The distribution of the eutrophication index across various stations provided profound insights into the nutrient enrichment and trophic status of the marine environment within the YSB (Figure 6). The distribution unveiled intricate patterns of nutrient enrichment and trophic status variation across the bay. The eutrophication index exhibited a broad range across the stations, spanning from 0.022 to 0.150, indicating a significant diversity in nutrient enrichment levels. Notably, station S2 emerged with the highest EI recorded as 0.150, signifying pronounced nutrient enrichment within that area. Conversely, station S12 displayed the lowest EI of 0.022, implying comparatively lower nutrient enrichment in comparison to other stations. Notably, all stations were classified as experiencing below the mild eutrophication level indicating the potentiality of lower eutrophication during the summer surface seawater of YSB. Furthermore, studies conducted by Jiang et al. (2019); Luo et al. (2022); Wei et al. (2022); Zhang et al. (2023); Zhou and Wang (2024), and Wang et al. (2022) on other seashores yielded similar results regarding eutrophication status, suggesting a dominance of mariculture and industrial activities alongside agricultural aspects within the YSB area. The distribution of EI hinted at localized zones with nutrient inputs, possibly

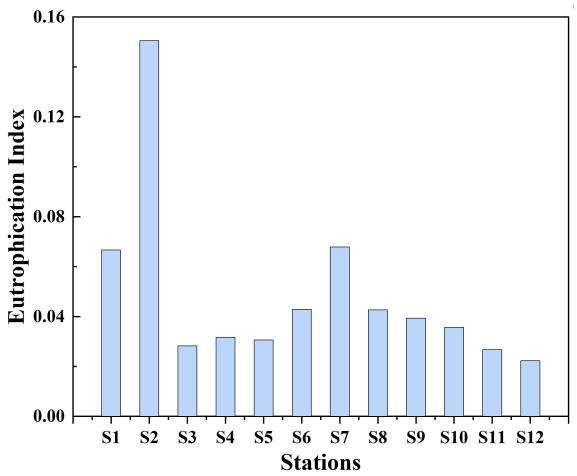

FIGURE 6
Distribution of eutrophication index of 2023 in the summer surface seawater of YSB, China.

influenced by anthropogenic activities such as urban runoff, sewage discharge, and residue from the seafood industry (Wang et al., 2012). These findings were consistent with decreasing trends observed from inshore to open sea, aligning well with previous studies on marine eutrophication (Liu et al., 2019; Zhang et al., 2023), which suggested that coastal areas adjacent to sewage treatment plants tend to exhibit higher nutrient enrichment levels due to the influx of excess nitrogen and phosphorus. Overall, the distribution of EI across the twelve stations in YSB unveiled patterns of nutrient enrichment diminished from inshore to offshore areas, highlighting localized zones of heightened nutrient inputs and varying levels of productivity throughout the study area.

3.4.2 Correlation of EI with dissolved nutrients and trace metals

Correlations between the eutrophication index (EI) and the concentrations of NO_2^-, NO_3^-, NH_4^+, PO_4^{3-}, DSi, TDN, Fe, Mn, Cu, and Zn are shown in Figures 7A–J as can be seen in eutrophication indices in the coastal waters of the YSB presented a positive correlation with nutrients and trace metals. NO_3^- concentrations exhibited a moderately positive correlation ($p > 0.05$, $n = 12$) suggesting a potential contribution to eutrophication processes within the bay. The presence of NO_3^-, often originating from agricultural runoff and wastewater discharge, can fuel algal blooms and subsequent oxygen depletion, exacerbating

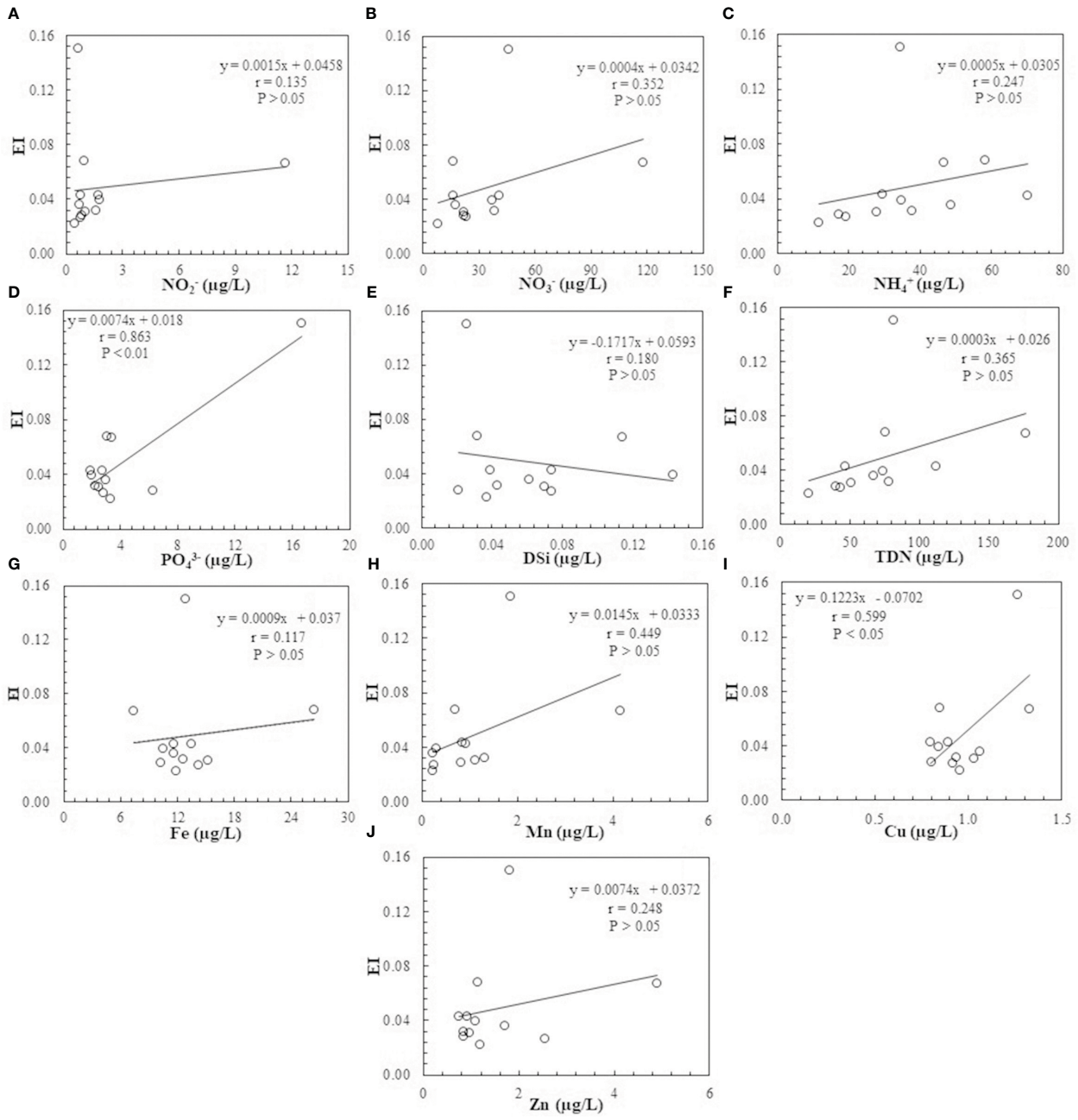

FIGURE 7
Correlation between nutrients **(A)** NO_2^-; **(B)** NO_3^-; **(C)** NH_4^+; **(D)** PO_4^{3-}; **(E)** DSi, **(F)** TDN; and trace metals **(G)** Fe; **(H)** Mn; **(I)** Cu; and **(J)** Zn with eutrophication index of 2023 in the summer surface seawater of YSB, China.

eutrophication (Wang et al., 2012, 2016). Conversely, NO_2^- displayed a weak positive correlation ($p > 0.05$, $n = 12$) indicating a less significant role in eutrophication status compared to NO_3^-. NH_4^+, though exhibited a positive correlation ($p > 0.05$, $n = 12$) that demonstrated a moderate significance, highlighting its potential contribution to nutrient enrichment and algal proliferation in the bay (Wang et al., 2012). Total dissolved nitrogen (TDN) also demonstrated a moderately positive correlation ($p > 0.05$, $n = 12$) reflecting its significance in driving nitrogen-driven eutrophication processes in coastal ecosystems (Zhang and Gao, 2016). All the data in the coastal YSB revealed that higher dissolved nitrogen concentrations were accompanied by lower EI. Furthermore, because nitrogen speciation can also affect the cell-size distribution of phytoplankton communities, the larger species may have the capacity for more internal storage of nutrients and become dominant in fluctuating nutrient regimes (Turpin and Harrison, 1979), and in general, smaller species have a higher preference for NH_4^- uptake over NO_3^- than larger phytoplankton species (Stolte et al., 1994), so different regions that have different sources and concentrations of Nitrogen compounds may have different species in making up the phytoplankton community. The knock-on effect was that the regions that have different sources and concentrations of N compounds may endure different degrees of eutrophication (Zhang and Gao, 2016). PO_4^{3-}, on the other hand, indicated a significant positive correlation ($p< 0.01$, $n = 12$) that suggested its pivotal role as a limiting nutrient in eutrophication processes. The prevalence of PO_4^{3-}, often sourced from agricultural runoff, sewage, and detergents, can fuel excessive algal growth, leading to detrimental ecological consequences such as hypoxia and biodiversity loss (Zhang and Gao, 2016). Dissolved silica (DSi) exhibited a moderate positive correlation indicating its potential role in supporting diatom growth and influencing nutrient cycling dynamics within the bay (Wang et al., 2012).

In addition, trace metals such as Fe, Mn, Cu, and Zn revealed intriguing relationships with eutrophication. Fe displayed a weak positive correlation ($p > 0.05$, $n = 12$) suggesting its potential role in catalyzing algal growth and modulating nutrient availability in seawater (Coale et al., 2004; Boyd et al., 2007). Mn exhibited a moderate positive correlation ($p > 0.05$, $n = 12$) indicating its influence on redox processes and nutrient cycling dynamics within the marine environment (Saito et al., 2005), as it is essential for photosynthesis and enzyme functions (Browning et al., 2021). High concentrations of Mn can stimulate phytoplankton growth by enhancing these physiological processes where excessive concentration can become toxic, leading to growth inhibition, demonstrating a complex balance in its impact on phytoplankton (Crawford et al., 2003; Saito et al., 2005). Cu demonstrated a significant positive correlation ($p< 0.05$, $n = 12$) highlighting its potential as a tracer for anthropogenic activities and its contribution to eutrophication processes through industrial discharges, food residue from mariculture, and chemical effluents from the port (Wang et al., 2012; Li et al., 2024). Cu can significantly reduce the phytoplankton diversity and productivity. However, limited bioavailability, due to low concentrations of labile compared to total Cu in the marine environment, may reduce exposure and the toxic effect (Rodgers et al., 2010). Zn though displayed a weak positive correlation ($p > 0.05$, $n = 12$) underscores its role as a potential cofactor in enzymatic processes and its significance in influencing nutrient enrichment in coastal ecosystems (Wang et al., 2012; Li et al., 2024).

Combining the above-mentioned data and discussions, it could be concluded that the enrichment of nutrients and trace metals may change eutrophication in the YSB but not considered as the higher trophic bay, suggesting that trace metals and nutrients were probably not the major reason for eutrophication elevation in the YSB, and changing the trace metals and nutrient concentration has limited effects on eutrophication in the YSB. However, the linkage between nutrient loading, eutrophication, and hypoxia/anoxia dynamics is often non-linear and complex in estuarine and coastal systems (Cloern, 2001). This is because these systems are hydrodynamically and biogeochemically distinct and highly variable. Climatic and physiographic differences between these systems affect profoundly physical–chemical and biological processes mediating organic matter production and accumulation, oxygen dynamics, nutrient cycling, and acidity (Zhang and Gao, 2016).

3.5 Comparative study

The mean concentrations of dissolved trace metals in surface seawater, namely Fe, Mn, Cu, and Zn, align with previous research findings (Supplementary Table S2) (Pan et al., 2020; Liang et al., 2022). Comparing these concentrations in YSB with other global and Chinese bays was presented in Table 1, it's noted that Fe levels in YSB were higher than in most regions, like those in Zhanjiang Bay (Hong et al., 2018) but lower than the Red Sea, Arabian Sea, and Abu-Qir Bay of Egypt (Al-Mur, 2020; Mohamed et al., 2021; Nishitha et al., 2023). Mn levels, however, were lower compared to Zhanjiang Bay, Pearl River Estuary, Red Sea, Arabian Sea, and Abu-Qir Bay of Egypt (Wang et al., 2012; Hong et al., 2018; Liu, 2019; Al-Mur, 2020; Mohamed et al., 2021; Nishitha et al., 2023). Cu concentrations exceeded those in Major River estuaries of East-Hainan (Fu et al., 2013) but were comparable to or lower than those in other regions. Similarly, Zn concentrations were higher than in the North Yellow Sea, and San Francisco Bay, USA (Flegal et al., 1991; Tian et al., 2009; Wang et al., 2022) but lower than in several other areas. Additionally, comparing nutrient and eutrophication index concentrations in YSB with other global and Chinese bays revealed that TDN levels were lower than in most regions but higher than in Tieshan Bay, Laizhou Bay, the North Yellow Sea, and Bay of Bengal, Bangladesh (Tian et al., 2009; Zhang and Gao, 2016; Wang et al., 2022; Alam et al., 2023; Zhang et al., 2023). The average TDP concentration in YSB was higher than in most bays but lower than in Tieshan Bay, Jinzhou Bay, and Red Sea (Al-Mur, 2020; Lin et al., 2020; Zhang et al., 2023). DSi levels in YSB were notably lower than in Laizhou Bay, Bay of Bengal, San Francisco Bay, and Red Sea (Flegal et al., 1991; Zhang and Gao, 2016; Al-Mur, 2020; Alam et al., 2023). Moreover, the eutrophication level, when compared to other bays, was significantly lower than in Tieshan Bay and the Pearl River Estuary (Wang et al., 2012; Liu, 2019; Zhang et al., 2023). Furthermore, concerning China's seawater quality standard, Cu,

10.3389/fmars.2024.1432566

TABLE 1 Comparison of three-year mean concentration (μg/L) of dissolved trace metals, nutrients, and eutrophication level in the summer surface seawater of YSB compared with other global and Chinese bays.

Region	Fe	Mn	Cu	Zn	TDN	TDP	DSi	EI	References
Jinzhou Bay, China	–	–	3.06 (1.26–6.49)	11.87 (1.58–25.73)	226.3	5.8	–	–	Lin et al. (2020)
Bohai Bay, China	–	–	0.16–7.17	17.3–90	246–1417	3.20–36.61	–	–	Peng (2015)
Tieshan Bay, China	–	–	–	–	71.0	8.00	–	0.519	Zhang et al. (2023)
Zhanjiang Bay, China	80.32 (60.28–108.4)	4.51 (3.05–7.54)	4.40 (3.35–7.03)	12.64 (5.71–25.70)	–	–	–	–	Hong et al. (2018)
Laizhou Bay, China	–	–	2.74 (1.63–4.31)	–	1.77 (0.074–7.08)	0.051 (0.0068–0.195)	3.05 (0.11–13.13)	–	Zhang and Gao (2016))
Pearl River Estuary, China	–	0.12–91.2	0.44–2.73	–	688.0	–	–	8.64	Wang et al. (2012); Liu (2019)
Major river estuaries of East-Hainan, China	2.23–535.7	–	0.15–1.21	–	–	–	–	–	Fu et al. (2013)
North Yellow Sea, China	–	–	0.80	3.80	19.85 (7.95–36.93)	3.68 (1.90–8.01)	–	–	Tian et al. (2009); Wang et al. (2022)
Yangtze River Estuary, China	6.06–35.86	–	1.22–1.68	–	–	–	–	–	Wang and Liu (2003)
Tianjin Coastal Area, China	–	–	6.98	24.83	–	–	–	–	Han et al. (2021)
Dingzi Bay, China	–	–	3.88	19.73	–	–	–	–	Pan et al. (2014)
Bay of Bengal, Bangladesh	–	–	27.47 (23.47–33.51)	44.53 (24.43–62.67)	0.62 (0.48–0.74)	0.12 (0.08–0.14)	7.65 (7.02–8.35)	–	Alam et al. (2023)
San Francisco Bay, USA	–	–	2.16	0.65	–	–	702.13–2106.41	–	Flegal et al. (1991); Cloern et al. (2017)
Red Sea, Saudi Arabia	29.33 (19.33–42.12)	1.56 (0.81–2.76)	1.67 (0.92–2.90)	22.02 (11.20–33.60)	560.14 (326.84–696.70)	51.72 (17.03–86.29)	115.57 (71.35–154.70)	–	Al-Mur (2020)
Arabian Sea, India	21.53 (17.95–27.41)	43.34 (6.20–113.98)	9.16 (6.40–14.90)	–	–	–	–	–	Nishitha et al. (2023)
Abu-Qir Bay, Egypt	14.50 (7.24–22.59)	5.72 (1.47–12.74)	1.432 (0.46–3.74)	12.01 (4.60–18.33)	–	–	–	–	Mohamed et al. (2021)
Grade I	–	–	<5	<20	<200	<15	–	–	SEPA (1997)
Grade II	–	–	<10	<50	<300	<30	–	–	SEPA (1997)
Grade III	–	–	<50	<100	<400	<45	–	–	SEPA (1997)
Yantai Sishili Bay	12.40 (4.79–26.71)	1.24 (0.19–6.41)	0.71 (0.26–1.53)	4.31 (0.74–13.12)	72.14 (20.26–176.26)	4.17 (1.90–16.68)	0.189 (0.021–0.714)	0.19 (0.022–0.150)	This Study

"-" represents no relevant reference data.
The parentheses present the range of the parameters' concentration.

Zn, TDN, and TDP concentrations adhered to Grade-I seawater quality standards in YSB (SEPA, 1997). Though there was no severe risk from trace metals, nutrient pollution, or potential eutrophication, control of the marine environment and ecosystems, as well as sustainable development, is needed to mitigate such threats. To effectively mitigate the potential threats (maybe) posed by nutrient and trace metal influx into YSB compared to other global and Chinese bays, several essential strategies should be implemented. Continuous and comprehensive monitoring of nutrient and trace metal levels in the bay is important, achieved through improved sample collection and analysis systems to ensure the accuracy and reliability of data.

Integration of advanced technologies like remote sensing and high-resolution modeling into monitoring programs can provide real-time data and predictive capabilities. Identifying and controlling pollution sources, including industrial discharges, agricultural runoff, and wastewater treatment processes, is crucial through stricter regulations. Promoting sustainable agricultural practices and effective waste management can further reduce pollution entering the bay. Addressing the ecological impacts of nutrient and trace metal influx in YSB requires a multi-faceted approach, including enhanced monitoring, pollution source control, habitat restoration, and community engagement, to maintain water quality and prevent severe eutrophication impacts

4 Conclusion

The spatial-temporal distribution and association with eutrophication, trace metals (Fe, Mn, Cu, and Zn), and nutrients (N, P, and Si) were investigated during summer surface seawater across 12 stations in YSB, located in Northern China. Significant variations in the distribution of trace metals and nutrients were observed, suggesting influences from anthropogenic pollution, discharged effluent, industrial and aquaculture activities, organismal uptake, and atmospheric deposition. Dissolved trace metals and nutrients displayed similar spatial-temporal patterns, indicating common influencing factors and sources, as revealed by correlation and PCA analysis. PC1 and PC2 collectively explained 98.1% of the total variance, with PC1 showing positive loading of Cu and other nutrient constituents, while PC2 indicated positive loading of Fe, Cu, NH_4^+, and PO_4^{3-}. Variations in trace metals and nutrient concentrations were noted across different years at all stations. Eutrophication distribution across the twelve stations revealed decreasing nutrient enrichment from inshore to offshore areas, indicating localized zones of heightened nutrient inputs and varying productivity levels. The linear relationship between eutrophication and trace metals, as well as nutrients, in the coastal waters, revealed a weak positive correlation with trace metals and a significant correlation with nutrients. As per the correlation analysis, nitrogen compounds were presumed to be the primary driving factor behind the fluctuations in eutrophication levels in this partially enclosed bay. Comparatively, the concentrations of trace metals, nutrients, and eutrophication in this bay were lower than those observed in other global and Chinese bays. Despite nutrient and trace metal concentrations generally meeting Grade-I seawater quality standards, there was a risk of contamination due to anthropogenic inputs from industrial effluent, waste discharge, sewage treatment plants, and mariculture operations. However, further research is needed to deepen understanding of the mechanisms underlying the relationship between trace metals, nutrients, and eutrophication. Therefore, this study offers valuable insights into the biogeochemical cycling process and distribution of nutrients, trace metals as well as eutrophication in the surface seawater of a typical bay in China.

Data availability statement

The original contributions presented in the study are included in the article/Supplementary Material. Further inquiries can be directed to the corresponding author.

Author contributions

MR: Conceptualization, Data curation, Formal analysis, Investigation, Methodology, Validation, Writing – original draft, Writing – review & editing. DP: Conceptualization, Funding acquisition, Methodology, Resources, Supervision, Validation, Writing – review & editing. YXL: Investigation, Writing – review & editing. YL: Investigation, Writing – review & editing.

Funding

The author(s) declare financial support was received for the research, authorship, and/or publication of this article. This work was financially supported by the National Natural Science Foundation of China (42177443), the Strategic Priority Research Program (XDB42000000) of the Chinese Academy of Sciences, the Taishan Scholar Project (tsqn202103133) of Shandong Province, and the Special Fund for the Scholar Program of Yantai City.

Conflict of interest

The authors declare that the research was conducted in the absence of any commercial or financial relationships that could be construed as a potential conflict of interest.

The author(s) declared that they were an editorial board member of Frontiers, at the time of submission. This had no impact on the peer review process and the final decision.

Publisher's note

Supplementary material

The Supplementary Material for this article can be found online at: https://www.frontiersin.org/articles/10.3389/fmars.2024.1432566/full#supplementary-material

References

Alam, M. J., Kamal, A. M., Ahmed, M. K., Rahman, M., Hasan, M., and Rahman, S. (2023). Nutrient and heavy metal dynamics in the coastal waters of St. Martin's island in the Bay of Bengal. *Heliyon* 9 (10), 20458. doi: 10.1016/j.heliyon.2023.e20458

Al-Mur, B. A. (2020). Assessing nutrient salts and trace metals distributions in the coastal water of Jeddah, Red Sea. *Saudi J. Biol. Sci.* 27, 3087–3098. doi: 10.1016/j.sjbs.2020.07.012

Boyd, P. W., Jickells, T., Law, C. S., Blain, S., Boyle, E. A., Buesseler, K. O., et al. (2007). Mesoscale iron enrichment experiments 1993–2005: synthesis and future directions. *Science* 315, 612–617. doi: 10.1126/science.1131669

Browning, T. J., Achterberg, E. P., Engel, A., and Mawji, E. (2021). Manganese co-limitation of phytoplankton growth and major nutrient drawdown in the Southern Ocean. *Nat. Commun.* 12, 884. doi: 10.1038/s41467-021-21122-6

Burger, H., Dickson, S., Awad, J., Marzouk, J., and Van Leeuwen, J. (2022). Investigation of cyanobacteria blooms in paper mill wastewaters and assessment of zinc as a control agent. *Int. J. Environ. Sci. Technol.* 19, 1105–1120. doi: 10.1007/s13762-021-03198-1

Cao, Z., Wang, D., Zhang, Z., Zhou, K., Liu, X., Wang, L., et al. (2020). Seasonal dynamics and export of biogenic silica in the upper water column of a large marginal sea, the northern South China Sea. *Prog. Oceanogr.* 188, 102421. doi: 10.1016/j.pocean.2020.102421

Chen, X., Li, T., Zhang, X., and Li, R. (2013). A Holocene Yalu River-derived fine-grained deposit in the southeast coastal area of the Liaodong Peninsula. *Chin. J. Oceanol. Limnol.* 31, 636–647. doi: 10.1007/s00343-013-2087-1

Cloern, J. E. (2001). Our evolving conceptual model of the coastal eutrophication problem. *Mar. Ecol. Prog. Ser.* 210, 223–253. doi: 10.3354/meps210223

Cloern, J. E., Jassby, A. D., Schraga, T. S., Nejad, E., and Martin, C. (2017). Ecosystem variability along the estuarine salinity gradient: Examples from long-term study of San Francisco Bay. *Limnol. Oceanogr.* 62, S272–S291. doi: 10.1002/lno.10537

Coale, K. H., Johnson, K. S., Chavez, F. P., Buesseler, K. O., Barber, R. T., Brzezinski, M. A., et al. (2004). Southern Ocean iron enrichment experiment: carbon cycling in high-and low-Si waters. *Science* 304, 408–414. doi: 10.1126/science.1089778

Couet, D., Pringault, O., Bancon-Montigny, C., Briant, N., Poulichet, F. E., Delpoux, S., et al. (2018). Effects of copper and butyltin compounds on the growth, photosynthetic activity and toxin production of two HAB dinoflagellates: The planktonic Alexandrium catenella and the benthic Ostreopsis cf. ovata. *Aquat. Toxicol.* 196, 154–167. doi: 10.1016/j.aquatox.2018.01.005

Crawford, D., Lipsen, M., Purdie, D., Lohan, M., Statham, P., Whitney, F., et al. (2003). Influence of zinc and iron enrichments on phytoplankton growth in the northeastern subarctic Pacific. *Limnol. Oceanogr.* 48, 1583–1600. doi: 10.4319/lo.2003.48.4.1583

Deppeler, S. L., and Davidson, A. T. (2017). Southern Ocean phytoplankton in a changing climate. *Front. Mar. Sci.* 4. doi: 10.3389/fmars.2017.00040

Derry, L. A., Kurtz, A. C., Ziegler, K., and Chadwick, O. A. (2005). Biological control of terrestrial silica cycling and export fluxes to watersheds. *Nature* 433, 728–731. doi: 10.1038/nature03299

Duan, L., Song, J., Li, X., Yuan, H., and Xu, S. (2010). Distribution of selenium and its relationship to the eco-environment in Bohai Bay seawater. *Mar. Chem.* 121, 87–99. doi: 10.1016/j.marchem.2010.03.007

Dugdale, R. C., Wilkerson, F. P., Hogue, V. E., and Marchi, A. (2007). The role of ammonium and nitrate in spring bloom development in San Francisco Bay. *Estuarine Coast. Shelf Sci.* 73, 17–29. doi: 10.1016/j.ecss.2006.12.008

Facey, J. A., Violi, J. P., King, J. J., Sarowar, C., Apte, S. C., and Mitrovic, S. M. (2022). The influence of micronutrient trace metals on Microcystis aeruginosa growth and toxin production. *Toxins* 14, 812. doi: 10.3390/toxins14110812

Faragallah, H., Tadros, H. R., and Okbah, M. (2010). Nutrient salts and chlorophyll-a during short term scale in the eastern harbor, alexandria (Egypt). *Malaysian J. Sci.* 29, 1–9. doi: 10.22452/mjs.vol29no1.1

Flegal, A., Smith, G., Gill, G., Sanudo-Wilhelmy, S., and Anderson, L. (1991). Dissolved trace element cycles in the San Francisco Bay estuary. *Mar. Chem.* 36, 329–363. doi: 10.1016/S0304-4203(09)90070-6

Fu, J., Tang, X.-L., Zhang, J., and Balzer, W. (2013). Estuarine modification of dissolved and particulate trace metals in major rivers of East-Hainan, China. *Continental Shelf Res.* 57, 59–72. doi: 10.1016/j.csr.2012.06.015

Gao, Y., Arimoto, R., Duce, R., Lee, D., and Zhou, M. (1992). Input of atmospheric trace elements and mineral matter to the Yellow Sea during the spring of a low-dust year. *J. Geophysical Research: Atmospheres* 97, 3767–3777. doi: 10.1029/91JD02686

Garmendia, M., Bricker, S., Revilla, M., Borja, Á., Franco, J., Bald, J., et al. (2012). Eutrophication assessment in Basque estuaries: comparing a North American and a European method. *Estuaries Coasts* 35, 991–1006. doi: 10.1007/s12237-012-9489-8

Han, X., Wang, J., Cai, W., Xu, X., and Sun, M. (2021). The pollution status of heavy metals in the surface seawater and sediments of the Tianjin coastal area, North China. *Int. J. Environ. Res. Public Health* 18, 11243. doi: 10.3390/ijerph182111243

Hong, Y., Zhang, J., Zhou, F., Chen, C., Sun, X., Shi, Y., et al. (2018). Spatial distribution and correlation characteristics of heavy metals in the seawater, suspended particulate matter and sediments in Zhanjiang Bay, China. *PloS One* 13, e0201414. doi: 10.1371/journal.pone.0201414

Hu, W., Yang, S., and Zhu, X. (2007). The impact of mariculture on the marine ecosystem and studies on bioremediation. *J. Xiamen Univ. (Natural Science)* 46, 197–202. doi: 10.1016/j.scitotenv.2016.05.004

Islam, M. S., and Tanaka, M. (2004). Impacts of pollution on coastal and marine ecosystems including coastal and marine fisheries and approach for management: a review and synthesis. *Mar. pollut. Bull.* 48, 624–649. doi: 10.1016/j.marpolbul.2003.12.004

Ji, Y., and Sherrell, R. M. (2008). Differential effects of phosphorus limitation on cellular metals in Chlorella and Microcystis. *Limnol. Oceanogr.* 53, 1790–1804. doi: 10.4319/lo.2008.53.5.1790

Jiang, Q., He, J., Wu, J., Hu, X., Ye, G., and Christakos, G. (2019). Assessing the severe eutrophication status and spatial trend in the coastal waters of Zhejiang province (China). *Limnol. Oceanogr.* 64, 3–17. doi: 10.1002/lno.11013

Jin, Z., Ding, S., Sun, Q., Gao, S., Fu, Z., Gong, M., et al. (2019). High resolution spatiotemporal sampling as a tool for comprehensive assessment of zinc mobility and pollution in sediments of a eutrophic lake. *J. Hazard. Mater.* 364, 182–191. doi: 10.1016/j.jhazmat.2018.09.067

John, S., and Sunda, W. (2019). *Trace metal nutrients*. doi: 10.1016/B978-0-12-409548-9.11648-3

Kalnejais, L. H., Martin, W. R., and Bothner, M. H. (2010). The release of dissolved nutrients and metals from coastal sediments due to resuspension. *Mar. Chem.* 121, 224–235. doi: 10.1016/j.marchem.2010.05.002

Kang, P., and Xu, S. (2016). The impact of mariculture on nutrient dynamics and identification of the nitrate sources in coastal waters. *Environ. Sci. pollut. Res.* 23, 1300–1311. doi: 10.1007/s11356-015-5363-0

Kelly, N. E., Guijarro-Sabaniel, J., and Zimmerman, R. (2021). Anthropogenic nitrogen loading and risk of eutrophication in the coastal zone of Atlantic Canada. *Estuarine Coast. Shelf Sci.* 263, 107630. doi: 10.1016/j.ecss.2021.107630

Lane, T. W., and Morel, F. M. (2000). A biological function for cadmium in marine diatoms. *Proc. Natl. Acad. Sci.* 97, 4627–4631. doi: 10.1073/pnas.090091397

Li, S. (2011). Interactions of Toxic Metals with Algal Toxins Derived from Harmful Algal Blooms. *FIU Electronic Theses and Dissertations* 478. doi: 10.25148/etd.FI11120206

Li, M., Bao, K., Wang, H., Dai, Y., Wu, S., Yan, K., et al. (2024). Distribution and ecological risk assessment of nutrients and heavy metals in the coastal zone of yantai, China. *Water* 16, 760. doi: 10.3390/w16050760

Li, Q., Legendre, L., and Jiao, N. (2015b). Phytoplankton responses to nitrogen and iron limitation in the tropical and subtropical Pacific Ocean. *J. Plankton Res.* 37, 306–319. doi: 10.1093/plankt/fbv008

Li, L., Liu, J., Wang, X., and Shi, X. (2015a). Dissolved trace metal distributions and Cu speciation in the southern Bohai Sea, China. *Mar. Chem.* 172, 34–45. doi: 10.1016/j.marchem.2015.03.002

Li, X., Wai, O. W., Li, Y. S., Coles, B. J., Ramsey, M. H., and Thornton, I. (2000). Heavy metal distribution in sediment profiles of the Pearl River estuary, South China. *Appl. Geochem.* 15, 567–581. doi: 10.1016/S0883-2927(99)00072-4

Li, W., Wang, Z., and Huang, H. (2020). Indication of size distribution of suspended particulate matter for sediment transport in the South Yellow Sea. *Estuarine Coast. Shelf Sci.* 235, 106619. doi: 10.1016/j.ecss.2020.106619

Li, L., Xiaojing, W., Jihua, L., and Xuefa, S. (2017). Dissolved trace metal (Cu, Cd, Co, Ni, and Ag) distribution and Cu speciation in the southern Yellow Sea and Bohai Sea, China. *J. Geophysical Research: Oceans* 122, 1190–1205. doi: 10.1002/2016JC012500

Liang, Y., Pan, D., Li, Y., Han, H., Wang, X., and Gai, G. (2024). Field determination and ecological health risk assessment of trace metals in typical mariculture area of China. *Mar. pollut. Bull.* 199, 115957. doi: 10.1016/j.marpolbul.2023.115957

Liang, Y., Pan, D., Wang, C., Lu, Y., and Fan, X. (2022). Distribution and ecological health risk assessment of dissolved trace metals in surface and bottom seawater of Yantai offshore, China. *Front. Mar. Sci.* 9. doi: 10.3389/fmars.2022.993965

Lin, H., Li, H., Yang, X., Xu, Z., Tong, Y., and Yu, X. (2020). Comprehensive investigation and assessment of nutrient and heavy metal contamination in the surface water of coastal Bohai Sea in China. *J. Ocean Univ. China* 19, 843–852. doi: 10.1007/s11802-020-4283-x

Lin, S., Litaker, R. W., and Sunda, W. G. (2016). Phosphorus physiological ecology and molecular mechanisms in marine phytoplankton. *J. Phycol.* 52, 10–36. doi: 10.1111/jpy.12365

Liu, X. (2019). *The variations of nutrients and phytoplankton assemblages in the bohai bay and their correlation analysis* (Beijing, China: Yantai Institute of Coastal Zone Research, University of Chinese Academy of Sciences). doi: 10.3390/jmse11081602

Liu, D., Keesing, J. K., Xing, Q., and Shi, P. (2009). World's largest macroalgal bloom caused by expansion of seaweed aquaculture in China. *Mar. pollut. Bull.* 58, 888–895. doi: 10.1016/j.marpolbul.2009.01.013

Liu, X., Liu, D., Wang, Y., Shi, Y., Wang, Y., and Sun, X. (2019). Temporal and spatial variations and impact factors of nutrients in Bohai Bay, China. *Mar. pollut. Bull.* 140, 549–562. doi: 10.1016/j.marpolbul.2019.02.011

Long, M., Holland, A., Planquette, H., Santana, D. G., Whitby, H., Soudant, P., et al. (2019). Effects of copper on the dinoflagellate Alexandrium minutum and its allelochemical potency. *Aquat. Toxicol.* 210, 251–261. doi: 10.1016/j.aquatox.2019.03.006

Long, M., Lelong, A., Bucciarelli, E., Le Grand, F., Hégaret, H., and Soudant, P. (2023). Physiological adaptation of the diatom Pseudo-nitzschia delicatissima under copper starvation. *Mar. Environ. Res.* 188, 105995. doi: 10.1016/j.marenvres.2023.105995

Longo, S., Sibat, M., Darius, H. T., Hess, P., and Chinain, M. (2020). Effects of pH and nutrients (nitrogen) on growth and toxin profile of the ciguatera-causing dinoflagellate Gambierdiscus polynesiensis (Dinophyceae). *Toxins* 12, 767. doi: 10.3390/toxins12120767

Lu, Y., Gao, X., Song, J., Chen, C.-T. A., and Chu, J. (2020). Colloidal toxic trace metals in urban riverine and estuarine waters of Yantai City, southern coast of North Yellow Sea. *Sci. Total Environ.* 717, 135265. doi: 10.1016/j.scitotenv.2019.135265

Lü, X., Qiao, F., Xia, C., Wang, G., and Yuan, Y. (2010). Upwelling and surface cold patches in the Yellow Sea in summer: Effects of tidal mixing on the vertical circulation. *Continental Shelf Res.* 30, 620–632. doi: 10.1016/j.csr.2009.09.002

Luo, Y., Liu, J.-W., Wu, J.-W., Yuan, Z., Zhang, J.-W., Gao, C., et al. (2022). Comprehensive assessment of eutrophication in Xiamen Bay and its implications for management strategy in Southeast China. *Int. J. Environ. Res. Public Health* 19, 13055. doi: 10.3390/ijerph192013055

Ma, X., Zuo, H., Tian, M., Zhang, L., Meng, J., Zhou, X., et al. (2016). Assessment of heavy metals contamination in sediments from three adjacent regions of the Yellow River using metal chemical fractions and multivariate analysis techniques. *Chemosphere* 144, 264–272. doi: 10.1016/j.chemosphere.2015.08.026

Manic, D. C., Redil, R. D., and Rodriguez, I. B. (2024). Trace metals in phytoplankton: requirements, function, and composition in harmful algal blooms. *Sustainability* 16 (12), 4876. doi: 10.3390/su16124876

Martin-Jézéquel, V., Hildebrand, M., and Brzezinski, M. A. (2000). Silicon metabolism in diatoms: implications for growth. *J. Phycol.* 36, 821–840. doi: 10.1046/j.1529-8817.2000.00019.x

Middag, R., De Baar, H. J., Bruland, K. W., and Van Heuven, S. M. (2020). The distribution of nickel in the west-Atlantic Ocean, its relationship with phosphate and a comparison to cadmium and zinc. *Front. Mar. Sci.* 7. doi: 10.3389/fmars.2020.00105

Mohamed, L., Salem, D., and Radwan, A. (2021). Evaluation of heavy metals pollution in seawater, suspended particulate matter and sediment from Abu-Qir Bay, Alexandria, Egypt. *Egypt. J. Aquat. Biol. Fish.* 25, 875–896. doi: 10.21608/ejabf.2021.170057

Morel, F., Milligan, A., and Saito, M. (2006). Marine bioinorganic chemistry: the role of trace metals in the oceanic cycles of major nutrients. *Oceans Mar. Geochem.* 6, 113. doi: 10.1016/B0–08-043751–6/06108–9

Nakaguchi, Y., Ikeda, Y., Sakamoto, A., Zheng, L., Minami, T., and Sohrin, Y. (2020). Distribution and stoichiometry of al, mn, fe, co, ni, cu, zn, cd, and pb in the east China sea. *J. Oceanogr.* 77, 463–485. doi: 10.1007/s10872-020-00577-z

Nishitha, D. S., Sudheer, A. K., Arun, K., Amrish, V. N., Mahesh, G., Udayashankar, H. N., et al. (2023). Risk assessment and spatio-temporal distribution of dissolved trace metals in Swarna, Sharavati and Kali estuaries, South-West Coast of India. *Environ. Sci. pollut. Res.* 30, 9914–9931. doi: 10.1007/s11356-022-22812-4

Paerl, H. W., Scott, J. T., Mccarthy, M. J., Newell, S. E., Gardner, W. S., Havens, K. E., et al. (2016). It takes two to tango: when and where dual nutrient (N & P) reductions are needed to protect lakes and downstream ecosystems. *Environ. Sci. Technol.* 50, 10805–10813. doi: 10.1021/acs.est.6b02575

Pan, D., Ding, X., Han, H., Zhang, S., and Wang, C. (2020). Species, spatial-temporal distribution, and contamination assessment of trace metals in typical mariculture area of north China. *Front. Mar. Sci.* 7. doi: 10.3389/fmars.2020.552893

Pan, J., Pan, J.-F., and Wang, M. (2014). Trace elements distribution and ecological risk assessment of seawater and sediments from Dingzi Bay, Shandong Peninsula, North China. *Mar. pollut. Bull.* 89, 427–434. doi: 10.1016/j.marpolbul.2014.10.022

Pavlidou, A., Simboura, N., Rousselaki, E., Tsapakis, M., Pagou, K., Drakopoulou, P., et al. (2015). Methods of eutrophication assessment in the context of the water framework directive: Examples from the Eastern Mediterranean coastal areas. *Continental Shelf Res.* 108, 156–168. doi: 10.1016/j.csr.2015.05.013

Peers, G., and Price, N. M. (2004). A role for manganese in superoxide dismutases and growth of iron-deficient diatoms. *Limnol. Oceanogr.* 49, 1774–1783. doi: 10.4319/lo.2004.49.5.1774

Peng, S. (2015). The nutrient, total petroleum hydrocarbon and heavy metal contents in the seawater of Bohai Bay, China: Temporal–spatial variations, sources, pollution statuses, and ecological risks. *Mar. pollut. Bull.* 95, 445–451. doi: 10.1016/j.marpolbul.2015.03.032

Redfield, A. C. (1958). The biological control of chemical factors in the environment. *Am. Sci.* 46, 230A–221.

Reich, H. G., Rodriguez, I. B., Lajeunesse, T. C., and Ho, T.-Y. (2020). Endosymbiotic dinoflagellates pump iron: differences in iron and other trace metal needs among the Symbiodiniaceae. *Coral Reefs* 39, 915–927. doi: 10.1007/s00338-020-01911-z

Rhodes, L., Selwood, A., Mcnabb, P., Briggs, L., Adamson, J., Van Ginkel, R., et al. (2006). Trace metal effects on the production of biotoxins by microalgae. *Afr. J. Mar. Sci.* 28, 393–397. doi: 10.2989/18142320609504185

Rodgers, K., Standing, D. B., Paton, G. I., Robinson, C. D., and Davies, I. M. (2010). Impact of copper on marine phytoplankton. *15th International Conference on Heavy Metals in the Environment*. (Poland: Department of Analytical Chemistry, Chemical Faculty, Gdansk University of Technology, Gdansk), 1071. doi: 10.3390/atmos10070414

Rue, E. L., and Bruland, K. W. (1995). Complexation of iron (III) by natural organic ligands in the Central North Pacific as determined by a new competitive ligand equilibration/adsorptive cathodic stripping voltammetric method. *Mar. Chem.* 50, 117–138. doi: 10.1016/0304-4203(95)00031-L

Saito, M. A., Noble, A. E., Hawco, N., Twining, B. S., Ohnemus, D. C., John, S. G., et al. (2017). The acceleration of dissolved cobalt's ecological stoichiometry due to biological uptake, remineralization, and scavenging in the Atlantic Ocean. *Biogeosciences* 14, 4637–4662. doi: 10.5194/bg-14-4637-2017

Saito, M. A., Rocap, G., and Moffett, J. W. (2005). Production of cobalt binding ligands in a Synechococcus feature at the Costa Rica upwelling dome. *Limnol. Oceanogr.* 50, 279–290. doi: 10.4319/lo.2005.50.1.0279

SEPA (1997). *The national standard of China for seawater quality (GB 3097–1997)* (Beijing: Standards Press of China).

Son, C. T., Giang, N. T. H., Thao, T. P., Nui, N. H., Lam, N. T., and Cong, V. H. (2020). Assessment of Cau River water quality assessment using a combination of water quality and pollution indices. *J. Water Supply: Res. Technology—AQUA* 69, 160–172. doi: 10.2166/aqua.2020.122

Stolte, W., Mccollin, T., Noordeloos, A. A., and Riegman, R. (1994). Effect of nitrogen source on the size distribution within marine phytoplankton populations. *J. Exp. Mar. Biol. Ecol.* 184, 83–97. doi: 10.1016/0022-0981(94)90167-8

Sun, Q., Liu, D., Liu, T., Di, B., and Wu, F. (2012). Temporal and spatial distribution of trace metals in sediments from the northern Yellow Sea coast, China: implications for regional anthropogenic processes. *Environ. Earth Sci.* 66, 697–705. doi: 10.1007/s12665-011-1277-4

Sun, X., Dong, Z., Zhang, W., Sun, X., Hou, C., Liu, Y., et al. (2022). Seasonal and spatial variations in nutrients under the influence of natural and anthropogenic factors in coastal waters of the northern Yellow Sea, China. *Mar. Pollut. Bull.* 175, 113171. doi: 10.1016/j.marpolbul.2021.113171

Sunda, W. (2006). Trace metals and harmful algal blooms. In *Ecology of harmful algae* (Berlin Heidelberg: Springer), 203–214. doi: 10.1007/978-3-540-32210-8

Sunda, W. G. (1994). Trace Metal/Phytoplankton Interactions in the Sea. In: G Bidoglio and W Stumm, editors. *Chemistry of Aquatic Systems: Local and Global Perspectives. EUROCOURSES*, vol 5. (Springer). doi: 10.1007/978-94-017-1024-4_9

Sunda, W. G., and Huntsman, S. A. (1998). Processes regulating cellular metal accumulation and physiological effects: phytoplankton as model systems. *Sci. Total Environ.* 219, 165–181. doi: 10.1016/S0048-9697(98)00226-5

Sunda, W. G., and Huntsman, S. A. (2000). Effect of Zn, Mn, and Fe on Cd accumulation in phytoplankton: Implications for oceanic Cd cycling. *Limnol. Oceanogr.* 45, 1501–1516. doi: 10.4319/lo.2000.45.7.1501

Tang, Q. (2004). "Study on ecosystem dynamics in coastal ocean," in *III, atlas of the resources and environment in the east China sea and the yellow sea ecosystem* (Science Press, Beijing, China).

Tian, L., Chen, H., Du, J., and Wang, X. (2009). Factors influencing distribution of soluble heavy metals in North Yellow Sea surface seawaters. *Ocean Univ. China* 39, 617–621.

Till, C., Shelley, R., Landing, W., and Bruland, K. (2017). Dissolved scandium, yttrium, and lanthanum in the surface waters of the N orth A tlantic: Potential use as an indicator of scavenging intensity. *J. Geophysical Research: Oceans* 122, 6684–6697. doi: 10.1002/2017jc012696

Tréguer, P. J., and De La Rocha, C. L. (2013). The world ocean silica cycle. *Annu. Rev. Mar. Sci.* 5, 477–501. doi: 10.1146/annurev-marine-121211-172346

Turpin, D. H., and Harrison, P. J. (1979). Limiting nutrient patchiness and its role in phytoplankton ecology. *J. Exp. Mar. Biol. Ecol.* 39, 151–166. doi: 10.1016/0022-0981(79)90011-X

Twining, B. S., and Baines, S. B. (2013). The trace metal composition of marine phytoplankton. *Annu. Rev. Mar. Sci.* 5, 191–215. doi: 10.1146/annurev-marine-121211-172322

Verschuren, D., Edgington, D. N., Kling, H. J., and Johnson, T. C. (1998). Silica depletion in Lake Victoria: sedimentary signals at offshore stations. *J. Great Lakes Res.* 24, 118–130. doi: 10.1016/S0380-1330(98)70804-4

Wagner, N. D., Quach, E., Buscho, S., Ricciardelli, A., Kannan, A., Naung, S. W., et al. (2021). Nitrogen form, concentration, and micronutrient availability affect microcystin production in cyanobacterial blooms. *Harmful Algae* 103, 102002. doi: 10.1016/j.hal.2021.102002

Wang, X., Cui, Z., Guo, Q., Han, X., and Wang, J. (2009). Distribution of nutrients and eutrophication assessment in the Bohai Sea of China. *Chin. J. Oceanol. Limnol.* 27, 177–183. doi: 10.1007/s00343-009-0177-x

Wang, C., Liang, S., Li, Y., Li, K., and Wang, X. (2015). The spatial distribution of dissolved and particulate heavy metals and their response to land-based inputs and tides in a semi-enclosed industrial embayment: Jiaozhou Bay, China. *Environ. Sci. pollut. Res.* 22, 10480–10495. doi: 10.1007/s11356-015-4259-3

Wang, Z.-L., and Liu, C.-Q. (2003). Distribution and partition behavior of heavy metals between dissolved and acid-soluble fractions along a salinity gradient in the Changjiang Estuary, eastern China. *Chem. Geol.* 202, 383–396. doi: 10.1016/j.chemgeo.2002.05.001

Wang, Y., Liu, Y., Chen, X., Cui, Z., Qu, K., and Wei, Y. (2022). Exploring the key factors affecting the seasonal variation of phytoplankton in the coastal Yellow Sea. *Front. Mar. Sci.* 9. doi: 10.3389/fmars.2022.1076975

Wang, Y., Liu, D., Dong, Z., Di, B., and Shen, X. (2012). Temporal and spatial distributions of nutrients under the influence of human activities in Sishili Bay, northern Yellow Sea of China. *Mar. pollut. Bull.* 64, 2708–2719. doi: 10.1016/j.marpolbul.2012.09.024

Wang, Y., Liu, D., Richard, P., and Di, B. (2016). Selection of effective macroalgal species and tracing nitrogen sources on the different part of Yantai coast, China indicated by macroalgal δ15N values. *Sci. Total Environ.* 542, 306–314. doi: 10.1016/j.scitotenv.2015.10.059

Wei, Y., Cui, H., Hu, Q., Bai, Y., Qu, K., Sun, J., et al. (2022). Eutrophication status assessment in the Laizhou Bay, Bohai Sea: further evidence for the ecosystem degradation. *Mar. pollut. Bull.* 181, 113867. doi: 10.1016/j.marpolbul.2022.113867

Wolfe-Simon, F., Grzebyk, D., Schofield, O., and Falkowski, P. G. (2005). The role and evolution of superoxide dismutases in algae 1. *J. Phycol.* 41, 453–465. doi: 10.1111/j.1529–8817.2005.00086.x

Xu, M., Wang, X., Xi, R., Long, Y., Kou, J., and Liu, X. (2018). Characteristics of nutrients and eutrophication assessment of shenzhen offshore waters. In *IOP Conference Series: Earth and Environmental Science* (IOP Publishing) 153 (6), 062038. doi: 10.1088/1755-1315/153/6/062038

Yano, K., Morinaka, Y., Wang, F., Huang, P., Takehara, S., Hirai, T., et al. (2019). GWAS with principal component analysis identifies a gene comprehensively controlling rice architecture. *Proc. Natl. Acad. Sci.* 116, 21262–21267. doi: 10.1073/pnas.1904964116

Yodsuwan, N., Sawayama, S., and Sirisansaneeyakul, S. (2017). Effect of nitrogen concentration on growth, lipid production and fatty acid profiles of the marine diatom Phaeodactylum tricornutum. *Agric. Nat. Resour.* 51, 190–197. doi: 10.1016/j.anres.2017.02.004

Yool, A., and Tyrrell, T. (2003). Role of diatoms in regulating the ocean's silicon cycle. *Global Biogeochem. Cycles* 17 (4). doi: 10.1029/2002GB002018

Youping, S., Junjie, Z., and Jianzhe, Q. (2020). Analysis of eutrophication trend of surface water in Tianjin coastal area. In *E3S Web of Conferences*, EDP Sciences, Vol. 206, 03002. doi: 10.1051/e3sconf/202020603002

Yuan, H., Song, J., Li, X., Li, N., and Duan, L. (2012). Distribution and contamination of heavy metals in surface sediments of the South Yellow Sea. *Mar. pollut. Bull.* 64, 2151–2159. doi: 10.1016/j.marpolbul.2012.07.040

Zhang, J., and Gao, X. (2016). Nutrient distribution and structure affect the acidification of eutrophic ocean margins: A case study in southwestern coast of the Laizhou Bay, China. *Mar. pollut. Bull.* 111, 295–304. doi: 10.1016/j.marpolbul.2016.06.095

Zhang, J., Huang, W., Liu, S., Liu, M., Yu, Q., and Wang, J. (1992). Transport of particulate heavy metals towards the China Sea: a preliminary study and comparison. *Mar. Chem.* 40, 161–178. doi: 10.1016/0304-4203(92)90021-2

Zhang, G., Liu, D., Wu, H., Chen, L., and Han, Q. (2012). Heavy metal contamination in the marine organisms in Yantai coast, northern Yellow Sea of China. *Ecotoxicology* 21, 1726–1733. doi: 10.1007/s10646-012-0958-4

Zhang, P., Wu, S., Xu, M., Luo, X., Peng, X., Ren, C., et al. (2023). Spatiotemporal nutrient patterns, stoichiometry, and eutrophication assessment in the tieshan bay coastal water, China. *J. Mar. Sci. Eng.* 11 (8), 1602. doi: 10.3390/jmse11081602

Zheng, Y., Jianhua, Q., and Manping, Z. (2003). The origin of iron in seawater and its relationship with phytoplankton. *Trans. Oceanol. Limnol.* 4, 38–48.

Zhou, B. (2018). Tendency and causes analysis of marine water quality of jinzhou bay. In *IOP Conference Series: Earth and Environmental Science* (IOP Publishing), Vol. 199, 022005.

Zhou, J., and Wang, Y.-S. (2024). A comprehensive approach to assessing eutrophication for the Guangdong coastal waters in China. *Front. Mar. Sci.* 10. doi: 10.3389/fmars.2023.1280821